Natural Resources Canada | Ressources naturelles Canada

GEOLOGICAL SURVEY OF CANADA
OPEN FILE 8842

CCGS Amundsen 2021805-806: marine geohazards, late Quaternary paleoenvironments, and seabed habitats in offshore Newfoundland and Labrador, and Nunavut, Canada

A. Normandeau, T. Carson, H. Sharpe, E. Edinger, B. Neves, and A. Belko

2022

Canada

GEOLOGICAL SURVEY OF CANADA
OPEN FILE 8842

CCGS Amundsen 2021805-806: marine geohazards, late Quaternary paleoenvironments, and seabed habitats in offshore Newfoundland and Labrador, and Nunavut, Canada

A. Normandeau[1], T. Carson[1], H. Sharpe[2], E. Edinger[3], B. Neves[4], and A. Belko[5]

[1] Geological Survey of Canada, 1 Challenger Drive, Dartmouth, Nova Scotia
[2] Department of Earth Sciences, University of New Brunswick, 3 Bailey Drive, Fredericton, New Brunswick
[3] Marine Institute, Memorial University of Newfoundland, Holyrood, 155 Ridge Road, St. John's, Newfoundland
[4] Fisheries and Oceans Canada, 80 East White Hills Road, St. John's, Newfoundland
[5] Centre de Recherche en Géomatique, Université Laval, 2325 Rue de l'Université, Québec, Quebec

2022

Permanent link: https://doi.org/10.4095/329213

This publication is available for free download through GEOSCAN (https://geoscan.nrcan.gc.ca/).

Recommended citation
Normandeau, A., Carson, T., Sharpe, H., Edinger, E., Neves, B., and Belko, A., 2022. *CCGS Amundsen 2021805-806*: marine geohazards, late Quaternary paleoenvironments, and seabed habitats in offshore Newfoundland and Labrador, and Nunavut, Canada; Geological Survey of Canada, Open File 8842, 51 p. https://doi.org/10.4095/329213

Publications in this series have not been edited; they are released as submitted by the author.

Table of Contents

LIST OF FIGURES

LIST OF TABLES

ACKNOWLEDGMENTS

We would like to thank Chief Scientists Maxime Geoffroy (Marine Institute, MUN) and Jean-Éric Tremblay (U. Laval) along with the entire ship crew led by Commanding Officers Alain Gariépy and Patrick Pellerin for continuous support in the execution of our scientific objectives. We also thank the governments of Nunavut and Nunatsiavut for permission to work in their marine territories.

Front cover. CCGS Amundsen in Southwind Fjord, Nunavut. Photo courtesy of David Cote (Fisheries and Oceans Canada)

1. BACKGROUND

This cruise supported two marine geoscience programs of the Geological Survey of Canada, the Public Safety Geoscience (PSG) and the Marine Geoscience for Marine Spatial Planning (MGMSP) programs. The cruise report mainly describes the operations conducted during 2021805 (CCGS Amundsen 2021 leg 2) but includes metadata for samples collecting during 2021806 (CCGS Amundsen 2021 leg 3). This report only addresses data collected for- and archived by- the Geological Survey of Canada.

1.1 Public Safety Geoscience

PSG has been conducting research to improve the understanding of geological processes and hazards (geohazards) in Baffin Bay to support stakeholder decisions on the use of offshore areas and provide northern communities with better knowledge for improving public safety. Since 2012, regional mapping of the Baffin Bay shelf and slope led to increased understanding on the distribution and timing of marine geohazards in the Arctic (Bennett et al., 2014; Jenner et al., 2018; Normandeau et al., 2018, 2020). However, many questions remain as to the exact mechanisms by which marine geohazards are triggered in the Arctic and their potential consequences on coastal communities and subsea infrastructure. Whereas much of NRCan's research from 2012 to 2018 focused on the offshore areas of Baffin Bay, relatively little effort had been spent examining the geohazard record preserved in fjords of Baffin Island. Fjords are known to be more susceptible to submarine and subaerial sidewall failures, producing some of the largest tsunamis on Earth. From the 14 largest tsunamis ever recorded, 10 occurred in glaciated environments such as fjords (Higman et al., 2018) in environments similar to Baffin Bay. The 2017 Greenland tsunami serves as a reminder of the risk they pose and their dramatic consequences on northern communities. As such, the Baffin Bay activity of PSG in collaboration with the ArcticNet Arctic Seafloor Mapping project, began working in Fjord environments (Broom et al., 2017; Normandeau et al., 2019a, 2019b, 2021a) to assess the triggers and frequency of active marine geohazards and the potential consequences they pose to Baffin Bay communities.

1.2 Marine Geoscience for Marine Spatial Planning

MGMSP conducts research on the marine geology of Canada's continental shelves. On the Canadian East Coast, the program focuses mainly on the Scotian Shelf and the Newfoundland Shelf. On the Labrador Shelf, research is being conducted to support Fisheries and Oceans Canada's decision-making on the use of the seabed. Therefore, high-resolution seabed mapping and ground-truthing of seabed sediment constitute the base map for properly managing seabed use.

2. OBJECTIVES

The main geological objective of the CCGS Amundsen (Fig. 1) 2021805 and 2021806 cruises were to collect seabed data along the northeastern Canadian Arctic and sub-Arctic. Specifically, the cruise aimed at:

1) In collaboration with the University of New Brunswick, Dalhousie University, Memorial University and DFO-Newfoundland, investigate Labrador shelf sediments, geomorphology, and paleoenvironments, through the use of seabed mapping and sediment core collection. Seabed data and cores collected during this cruise will aim at reconstructing past nearshore environments, such as sea-ice conditions, current strength over time and storm frequency. The geomorphology of the shelf, characterized with the use of a multibeam echosounder, will aim at identifying hotspots of seabed habitats along the Makkovik/Nain region.
2) Opportunistic mapping and sediment coring for marine geohazards along the Labrador Shelf and Hudson Strait continental slope. Submarine landslides are prevalent along the continental slope (Kostylev et al., 2020) and the collection of sediment cores will help understand their timing and trigger mechanisms.
3) Continue the Southwind Fjord marine geohazard experiment (see Normandeau et al., 2021) through the recovery of a mooring deployed in 2019 during *2019Nuliajuk* (Normandeau et al., 2019b) and the deployment of a remotely-operated vehicle (ROV) on a submarine landslide triggered in 2018 by an iceberg (Normandeau et al., 2021b). These data will help characterize and understand the causes of modern marine geohazards in Baffin Bay.
4) In collaboration with Laval University, investigate the retreat history of the Laurentide Ice Sheet on the Baffin Bay Shelf to better characterize seabed sediments and their distribution.
5) Investigate the unexpected presence of a small turbidity current system offshore Scott Inlet. Sediment cores collected on this system will help understand the causes of marine geohazards in an area of the seafloor where such processes are unexpected.
6) In collaboration with Dalhousie University and through the ULLINIQ project (Gosse et al., 2020), investigate subaerial to marine landslides in Scott and Gibbs Fjord in order to evaluate the hazard they pose to northern communities. An integrated subaerial, with

uncrewed aerial vehicle, and marine dataset will be used to understand the wide range of geohazards affecting glacierized fjords.

Figure 1: The CCGS Amundsen at the entrance of Southwind Fjord. Photo courtesy of David Cote (DFO).

3. SUMMARY OF ACTIVITIES

The 2021805 cruise began in St. John's, Newfoundland, on July 15 and ended in Iqaluit on August 12, 2021. The full cruise track is available in Figure 2. The vessel visited nine different sites where seabed data was collected and archived at the Geological Survey of Canada.

The 2021805 and 2021806 cruise allowed the collection of:

1) 9 piston cores
2) 8 giant gravity cores
3) 4 small gravity cores
4) 13 box cores
5) 1 CTD profile
6) 1 mooring recovery
7) 2 ROV dives

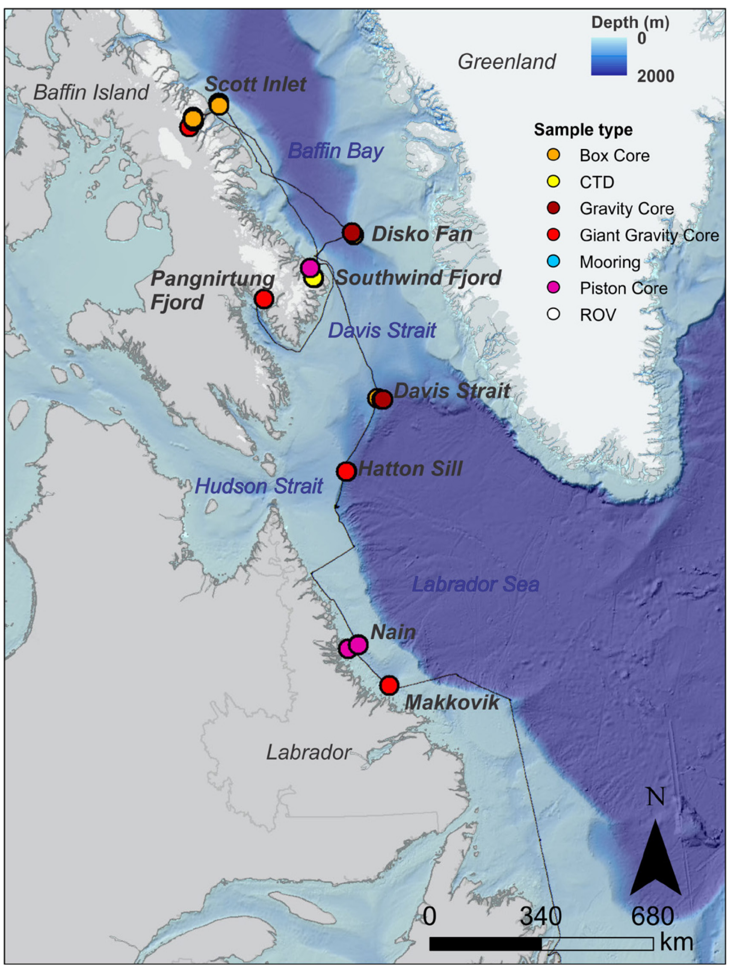

Figure 2: Navigation lines of the 2021805 cruise.

4. Preliminary Results

4.1 Labrador Shelf

In the Makkovik area of the Labrador shelf, multibeam mapping revealed the presence of glacial lineations on the seafloor associated with the passage of an ice stream during the last glaciation. In addition, bedrock outcrops with steep-side slopes are visible in the imagery (Fig. 3). Three ROV dives on those steep-sided slopes revealed the presence of coral habitats. The multibeam imagery suggested that steep-sloped bedrock habitats are widespread along the Makkovik and Nain troughs.

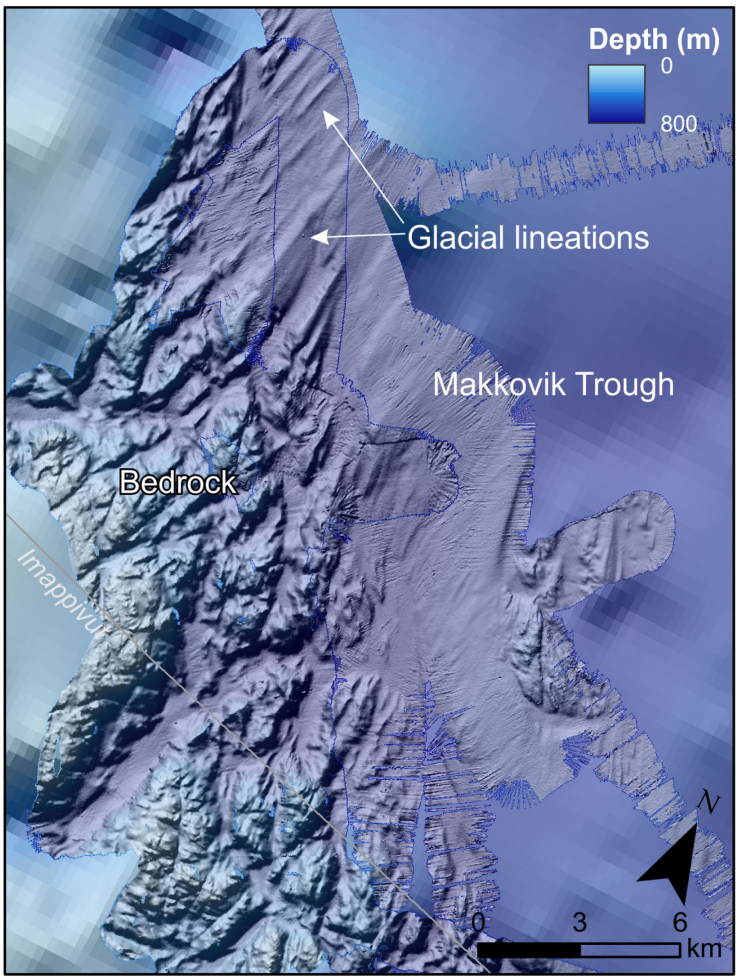

Figure 3: Geomorphology of upper Makkovik Trough illustrating highly dissected glacially-carved bedrock and glacial lineations. See location in Fig. 2.

In the Nain area, a series of channels and islands constrict water masses and produces strong near-bed currents. These currents erode surficial sediments in many places, preventing the continuous deposition of mud over time. However, in the Nain trough adjacent to the Nain bank, a drift system is visible on a sub-bottom profile (Fig. 4). This drift system is characterized by a moat, where near-bed currents are focused, a mounded drift, where sediment accumulates over time depending on current strength, and a plastered drift on the Nain bank where sediment thins towards the top of the bank. The presence of a drift system in the area and the collection of a sediment core (2021805-005, see appendix B) on the mounded drift should allow us to reconstruct flow strength over time.

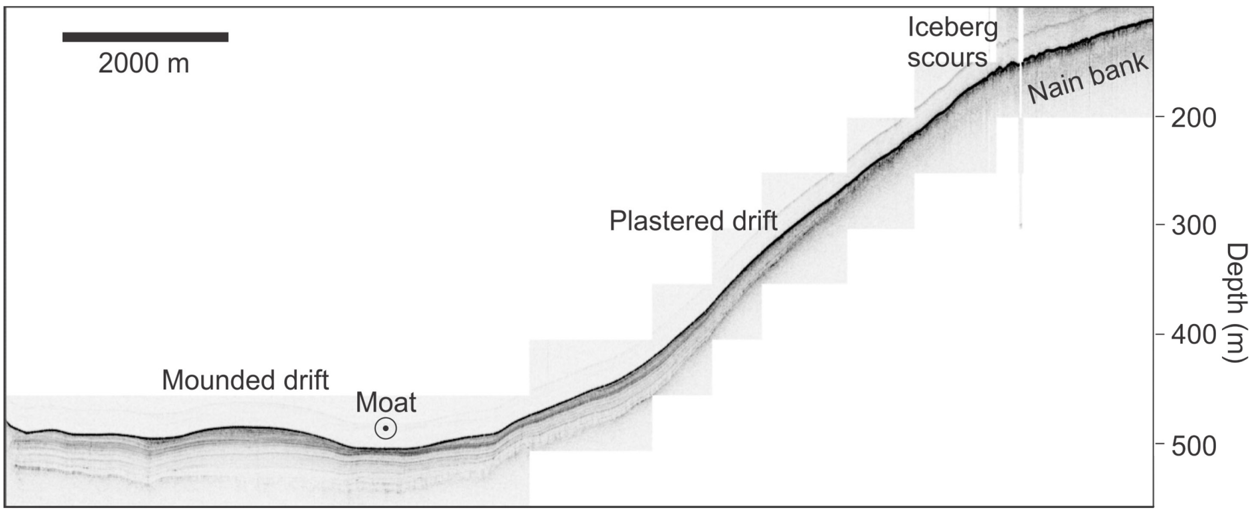

Figure 4: Drift deposits in the Nain Trough.

4.2 Southwind fjord

The Southwind Fjord geohazard monitoring was built on initial seabed mapping done in 2013 and 2014 by ArcticNet (Hughes-Clarke et al., 2015) that showed the presence of a submarine channel and many submarine landslides on the steep sidewalls of the fjord. In 2018, a CCGS Hudson expedition allowed further study of the fjord by collecting numerous sediment cores on the fjord sidewalls and repeat seabed mapping to assess changes on the seabed (Normandeau et al., 2018). This experiment continued with a mooring deployed in 2019 from the RV Nuliajuk (Normandeau et al., 2019b). Repeat multibeam mapping of the system during CCGS Amundsen 2021805 showed that sediment waves in the channel, called cyclic steps (Ghienne et al., 2021), migrated upslope between 2019 and 2021 (Fig. 5). Preliminary interpretation of Conductivity-Temperature-Depth (CTD) data from the mooring shows that turbidity increases markedly during the spring and summer months (Fig. 5), indicating that glacial meltwaters provide large volumes of sediment to the fjord. The analysis of the mooring data will allow to understand the exact timing of turbidity currents in the fjord in relation to glacial melt.

An ROV dive was also completed on the 2018 iceberg-triggered landslide (Normandeau et al., 2021b). ROV imagery quality was impacted by high sediment turbidity in the water column, but observations were still possible. The imagery revealed the presence of numerous displaced blocks, small-scale thrusting, and iceberg impact on the seabed (Fig. 6). An intact piece of kelp was also sampled with the ROV. Most of these features appeared slightly draped with mud, indicating relatively high sedimentation rates since 2018.

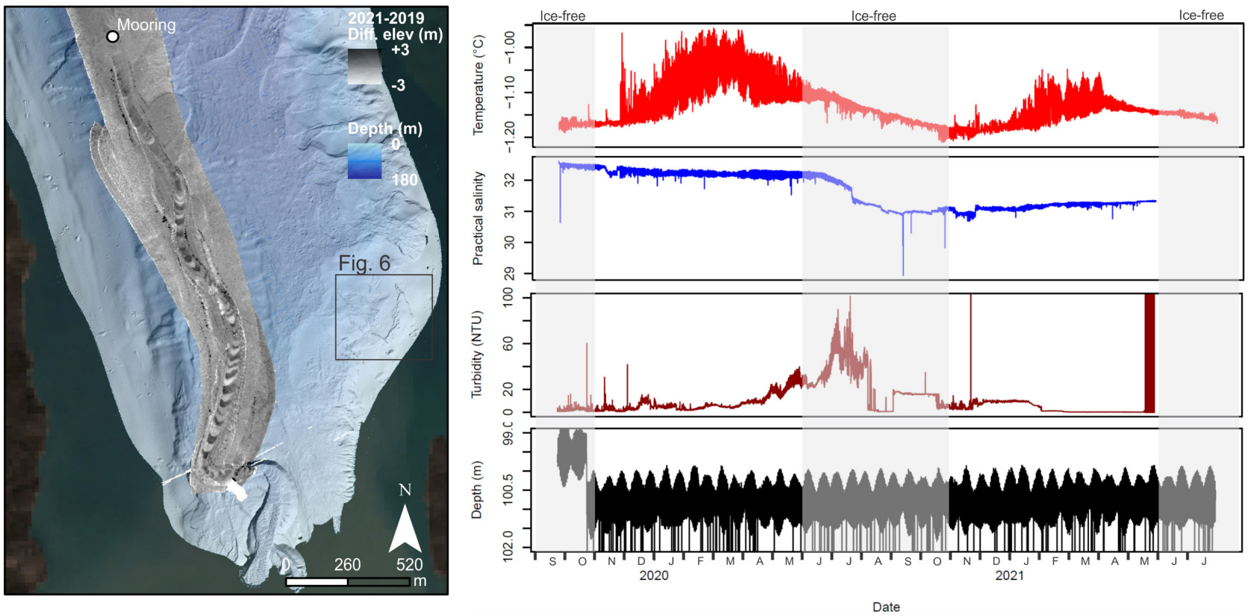

Figure 5: Raw CTD data collected at a water depth of 100 m in Southwind Fjord, from September 2019 to July 31, 2021.

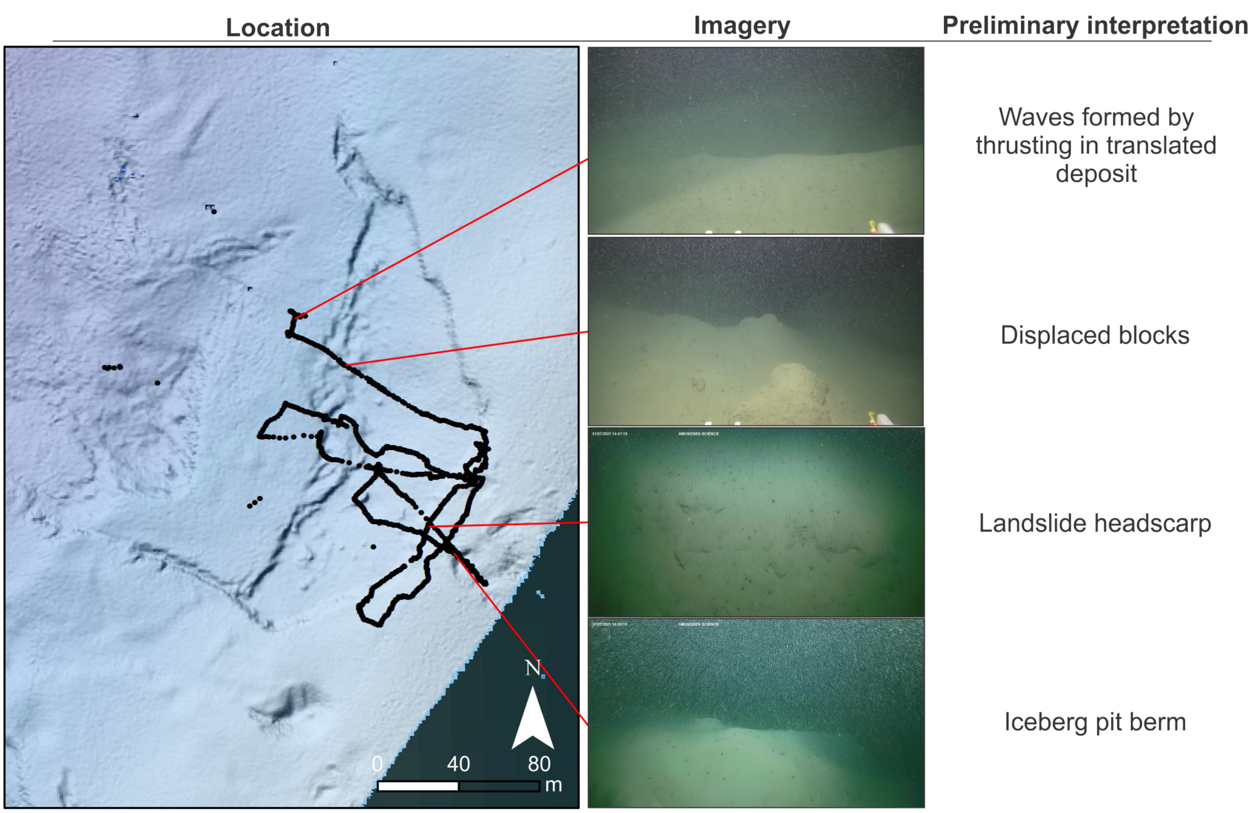

Figure 6: ROV dive on the 2018 submarine landslide in Southwind Fjord.

4.3 Scott Inlet

In Scott Inlet, a series of submarine channels and sediment waves are visible on the seafloor on the edge of a large glacial trough. This system, previously imaged in Bennett et al. (2014), is located 40 km away from land and begins at a water depth of 200 m. Similar submarine channels are generally associated river deltas or longshore drift; therefore, they are generally within 1 km of the coast and in shallow waters. This system thus appears out of place since it is far from a source of coastal sediment. During the cruise, the opportunity of mapping this system (Fig. 7A) to identify changes on the seabed, collecting sediment cores and completing a short ROV dive presented itself. Sediment cores collected on the system using a box core and the ROV push-corer showed that sand is buried under ≤10 cm of mud (Fig. 7B). In this system, the sandy layer is interpreted as a turbidite resulting from the activity of the submarine channels. The presence of a turbidite close to the seabed indicates that this system was active relatively recently, during the mid-to late-Holocene. Radiometric dating of the sediment will precise the exact age of the last turbidity current passing through the system. In addition, the ROV dive revealed very steep, near vertical walls at the head of the submarine channels and carbonate crusts suggestive of seepage in the area (Cramm et al., 2021). These walls were covered with crinoids (sea feathers) in very high densities (Figure 7C-F). Taken together, these data will allow us to understand the presence of these submarine channels offshore Scott Inlet.

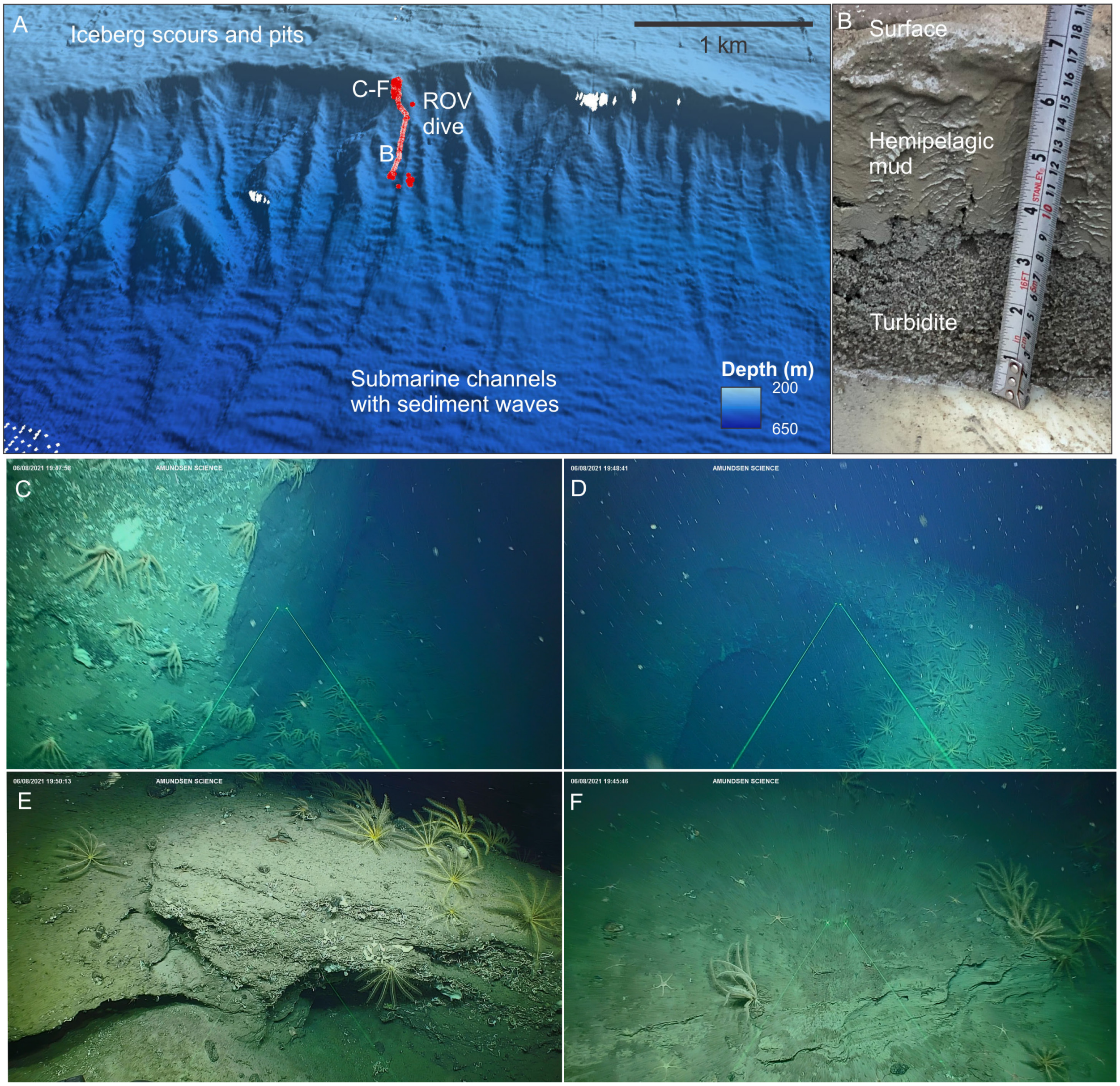

Figure 7: Results from the Scott Inlet submarine channel study. A) Multibeam bathymetry of the ROV dive area; B) Box core sample collected in a submarine channel showing a turbidite 10cm below hemipelagic mud; C-F) Images from the ROV illustrating the steep headwalls and carbonate crusts at the head of the channels. Green laser dots are 10 cm apart. See figure B24 for location of A.

4.4 Piston- and gravity coring of deep-sea coral habitats in Davis Strait and Disko Fan.

Two species of bamboo corals with carbonate skeletons form biogenic habitats on soft sediment in the Northwest Atlantic. Habitats of the larger bamboo coral, *Keratoisis* cf. *flexibilis*, have been previously described on the Disko Fan (de Moura Neves et al., 2015), where they form small mounds by trapping hemipelagic sediment. These mounds were first cored from the Amundsen in 2016, and found a minimum habitat longevity of ~2 ka (Edinger et al., 2017). During the

Amundsen 2021 cruise, additional piston and gravity coring targeted biogenic habitats formed by both *Keratoisis* and a smaller species of bamboo coral, *Acanella arbuscula*, at the Davis strait site.

At both sites, 3.5 kHz sub-bottom profiles were collected following the track of an ROV dive, enabling targeted coring of these habitats. Cores 2021805-011 and 2021805-012 targeted habitats associated with the small bamboo coral, *Acanella arbuscula*. Cores 2021805-020, 2021805-021 and 2021805-022 targeted habitats built by the larger bamboo coral, *Keratoisis* sp. Core recovery details are presented in Appendix A.

5. EQUIPMENT AND PROCEDURES

5.1 Knudsen 3260 Echo-Sounder

In May 2016, a Knudsen 3260 deck unit was installed onboard the Amundsen. It was acquired to replace the old 320-BR system that had shown signs of high degradation at the end of the 2015 field season. The new system operated using a USB connector instead of a SCSII communication port. Sub-bottom profiles were acquired along transits at a frequency of 3.5 kHz to image sub-bottom stratigraphy of the seafloor.

5.2 EM-302 multibeam echosounder

The Amundsen is equipped with an EM302 multibeam sonar operated with the *Seafloor Information System* (SIS). Attitude is given by an *Applanix POS-MV* receiving RTCM corrections from a *CNAV 3050* GPS receiver. Position accuracies were approximatively < 0.8m in planimetry and < 1m in altimetry. Beam forming at the transducer head is done by using an *AML* probe. CTD-Rosette casts, when available, were used for sound speed corrections.

All the data acquired during the cruise were post-processed in real-time using the CARIS HIPS&SIPS 11.1 software. This post-processing phase is essential to rapidly detect any anomaly in the data collection. The final addition of the 2021 data will be done upon the return of the ship in Quebec City.

5.3 *Coring*

During the cruise, four types of coring equipment were used: 1) Piston core (PC); 2) Giant gravity core (GGC); 3) Gravity core (GC); 4) Box core (BC). ROV push-cores were deployed at one location (Scott Inlet), but are described in session 5.5. The piston core uses the 900lbs core head with three barrels and a trigger weight core (or pilot core) as a trigger (Fig. 8A). When time was limited, the 900 lbs core head with three barrels was used with a butterfly valve, which allowed it to be used as a 9m gravity core instead of as a piston core (Fig. 8B). This setup saved approximately 30-45 minutes per deployment and was therefore useful when multiple operations needed to be done during daytime. The small gravity core (Fig. 8C) was used when time was more limited (≤ 1h) since it requires less operations on deck.

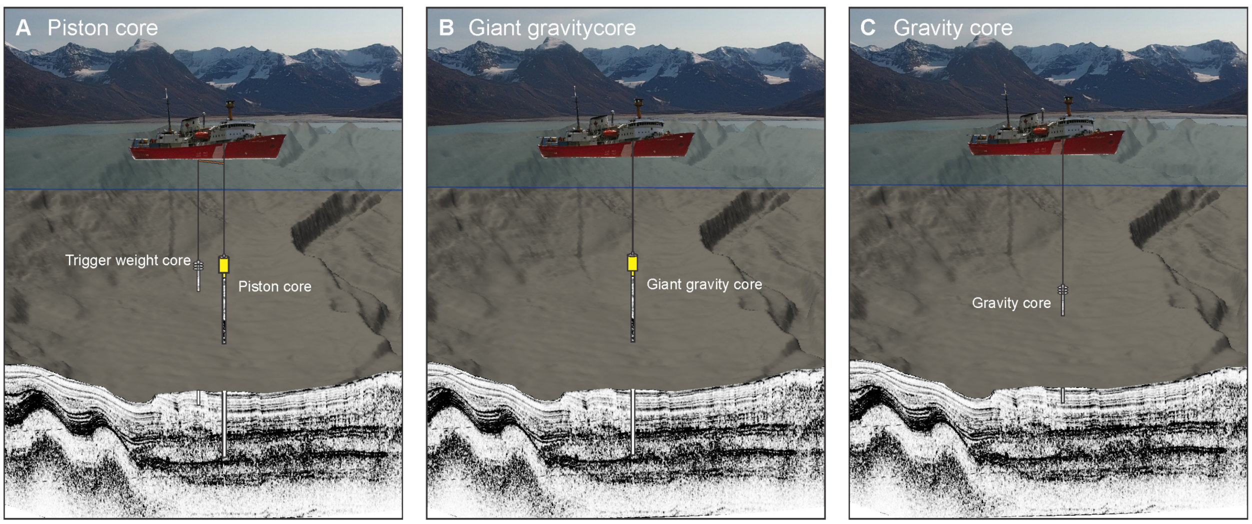

Figure 8: Types of coring equipment used during the 2021805 cruise.

5.3.1 Onboard gravity core processing and subsampling

A total of 31 cores (7 PC and 8 GGC, 3 GC and 13 BC) were collected during the cruise 2021805 and 4 cores during 2021806 (2PC, 1GC and 1BC). All cores were processed according to standard GSC Atlantic core procedures (Mudie et al., 1984). All core barrels were kept in sequence, from the bottom to the top, as the barrels were taken apart. Starting with the bottommost barrel each 10 ft length of liner was extruded from the barrel and cut in half, using a modified pipe cutter. The sediment in the liner was cut using a wire saw and the section ends were carefully capped to minimize disturbance to the sediment surface. The top end cap of each section was labelled with the cruise number, station number, section label, and as the top. The base of the piston core was designated as "A Base" and the top of the base section was designated as "B Top". The base of the following section was designated as "B Base" and the top of the section was designated as "C Top". This labelling system continued until all sediment was sectioned. All sections were then taken into the geology lab and labelled with an arrow indicating the upwards direction, as well as the cruise number, station number, and their respective sections labels (AB, BC, etc.). End caps were removed if the sediment was not too fluid, and the section length was measured and recorded.

The sealed core sections were stored upright in custom-made whole core portable racking units in the starboard refrigerated reefer container and maintained at 4°C. All core cutters and catchers were measured, labelled, placed in split liners, waxed and stored upright in buckets in the reefer container.

All station location information, core section lengths, extruded pieces and cutter/catcher lengths, sediment description, core performance information and all relevant field information were documented on deck sheets. Summary of core sections are available in Appendix A.

5.3.2 Physical properties measurements

Undrained shear strength measurements and constant volume samples were taken at the ends of each section if the condition of the sediment allowed (Table 1-2). The constant volume sampler was inserted into the end of the section, the undrained shear strength measurement was taken and then the constant volume sampler was removed.

The undrained shear strength was measured using a hand-held Hoskin Scientific Torvane according to ASTM Test Method D2573 Field Vane Shear Test in Saturated Fine Grained Soil. The dial on the Torvane was zeroed, the fins on the vane were gently pushed into the sediment until they were completely inserted. The Torvane was rotated at a constant rate until the sediment failed.

The Torvane dial reading ranges from 0 to 1 and reports values in kg-force/cm^2 units (1 kg/cm^2 = 98.07 kPa). The Torvane has three adapter vanes as described below:

L - Sensitive vane has a range of 0 to 0.2 Kg-force/cm^2

Su = dial reading * 0.2 Kg-force/cm^2

M - Regular vane has a range of 0 to 1.0 Kg-force/cm^2

Su = dial reading * 1 Kg-force/cm^2

S - High capacity vane has a range of 0 to 2.5 Kg-force/cm^2

Su = dial reading * 2.5 Kg-force/cm

The L - Sensitive vane was used for a total of 31 undrained shear strength measurements taken during the cruise.

Constant volume samples for bulk density and water content determinations were taken by inserting stainless steel samplers of a known volume. Prior to insertion, the sampler was lightly sprayed with mineral oil and gently wiped with a small Kimwipe tissue. The bevelled edge of the sampler was placed on the flat sediment surface and the carefully inserted into the sediment using two flat-headed spatulas. The sampler is inserted at a constant rate to minimize compression of the sediment within the sampler. The sampler was then carefully removed and the sediment was trimmed using a wire saw and extruded into a pre-weighed 1 oz screw-top glass bottle. The bottle cap was then labelled and sealed using electrical tape to prevent the lid from loosening. A total of 29 constant volume samples were taken during the cruise. The samples will be weighed, dried at 105°C for 24 hours and reweighed to determine bulk density, dry density and water content according to ASTM Test Method D 2216 Laboratory Determination of Water (moisture) Content of Soil and Rock by Mass. All relevant information for the Torvane measurements and constant volumes was recorded on data sheets and input into excel spreadsheets and will be incorporated into the GSC Atlantic physical property database.

Table 1: Summary of Torvane measurements

Station No.	Sample Type	Section	Top/Base	Vane used	Reading
001	GGC	AB	Top	L	6
001	GGC	BC	Top	L	5.5
001	GGC	BC	Base	L	4
001	GGC	CD	Top	L	3
001	GGC	CD	Base	L	4
001	GGC	DE	Base	L	3.25
003	PC	AB	Top	L	4.5
003	PC	BC	Top	L	5
003	PC	AB	Base	L	3
003	PC	BC	Base	L	3.5
003	PC	CD	Base	L	3.2
005	PC	AB	Top	L	4
005	PC	BC	Top	L	4.5
005	PC	CD	Top	L	3.25
005	PC	BC	Base	L	4
005	PC	DE	Base	L	3
019	PC	AB	Top	L	5
019	PC	BC	Top	L	1.5
019	PC	CD	Top	L	2.5
019	PC	DE	Top	L	0.25
019	PC	BC	Base	L	3.5
019	PC	CD	Base	L	2.5
019	PC	DE	Base	L	2.7
023	PC	BC	Base	L	2
023	PC	AB	Top	L	0.25
023	PC	AB	Top	L	0.25
025	PC	AB	Top	L	0.25

29	GGC	AB	Top	L	0
29	GGC	BC	Base	L	0
29	GGC	BC	Top	L	0.5
30	GGC	AB	Top	L	0.25

Table 2: Summary of constant volume sampling

Station No.	Sample Type	Section	Top/Base	Sampler ID	Bottle ID
001	GGC	AB	Top	A4	A91
001	GGC	BC	Top	A5	A21
001	GGC	BC	Base	A6	A47
001	GGC	CD	Top	A7	A192
001	GGC	CD	Base	A8	A191
001	GGC	DE	Base	A9	A22
003	PC	AB	Top	A2	A9
003	PC	BC	Top	A2	A44
003	PC	AB	Base	A2	A23
003	PC	BC	Base	A2	A149
003	PC	CD	Base	A2	A18
005	PC	AB	Top	A2	A32
005	PC	BC	Top	A2	A45
005	PC	CD	Top	A2	A5
005	PC	BC	Base	A2	A176
005	PC	DE	Base	A2	A37
019	PC	AB	Top	A2	A165
019	PC	BC	Top	A2	A156
019	PC	CD	Top	A2	A54
019	PC	DE	Top	A2	A51
019	PC	BC	Base	A2	A27
019	PC	CD	Base	A2	A56
019	PC	DE	Base	A2	A161
023	PC	BC	Base	A4	A189
023	PC	AB	Top	A4	A3
029	GGC	AB	Top	A4	A174
029	GGC	BC	Base	A5	A14

029	GGC	BC	Top	A6	A12
030	GGC	AB	Top	A7	A48

5.4 Mooring

5.4.1 Mooring design

The mooring deployed during *2019Nuliajuk* (Normandeau et al., 2019b) was successfully recovered during this cruise. The mooring consisted of a 825 lbs train-wheel, 5 m of chain to the acoustic release, followed by the following instruments (Fig. 9):

1- Five HOBO temperature sensors were spread out on the line to measure variability in temperature near the bottom.
2- Halfway up on the line, a Seametrics CT2X measures both temperature and conductivity.
3- At 19 m above bottom, a RBR concerto3 CTD-Tu was installed and measures conductivity, temperature, depth and turbidity.
4- At 21 m above bottom, a Nortek Signature 500 ADCP is positioned to look downward. The ADCP has five beams but is set-up to use only 4 beams since the line interacts with the 5th beam.

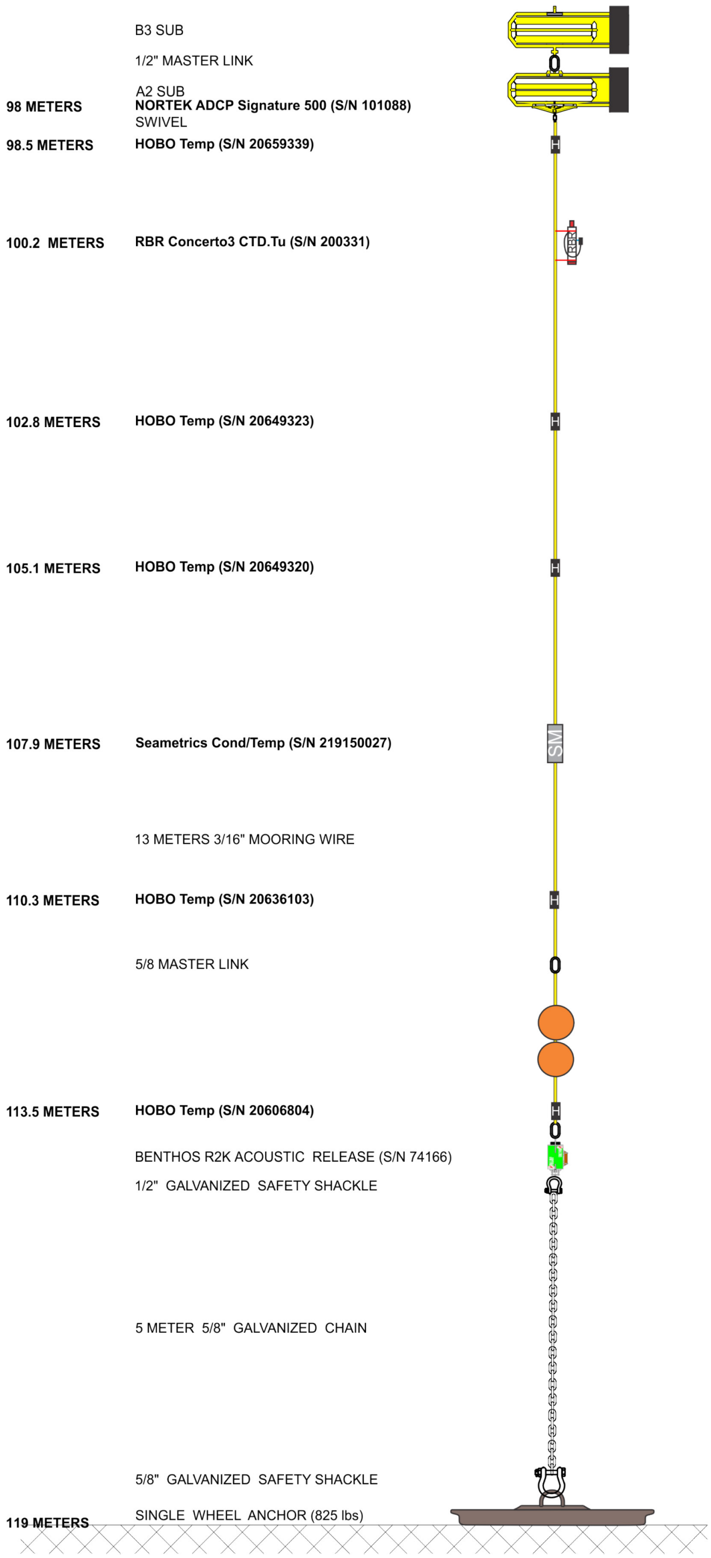

Figure 9: Mooring design combining the downward-looking ADCP, 5 HOBO temperature sensors, 1 RBRConcerto CTD-Tu and 1 Seametrics CT2X CT.

5.4.2 Mooring recovery

Minor issues were encountered during the recovery of the mooring. Communications with the acoustic release failed the first five attempts. Therefore, the ship moved to another position to attempt a sixth time to communicate with the acoustic release. When changing position, communication was successful. Since communication with the acoustic release was unstable, it was decided not to triangulate the mooring and to immediately release it in order to avoid losing communications once more. Triangulation was not necessary since the mooring was observed on the EM302 water column imagery (Table 3, Fig. 10). Upon recovery of the mooring, all data was recovered from the instruments in order to validate that they worked properly (Table 4). The HOBOs and RBR CTD worked as programmed whereas an apparent battery failure prevented the ADCP of recording data after June 3rd 2020. The CT2X flooded and no data could be recovered.

Table 3: Position of the mooring estimated using the water column display of the EM302

ID	Latitude	Longitude	Depth (m)	Time (UTC)
Mooring from MBES	66.761698	-62.339844	120	212/11:29

Table 4: Details on instrument records

Instrument	Start day/time	End day/time	Comments
ADCP Signature 500	September 23, 2019	June 3, 2020	Was supposed to last until November 2020 (500 days) but did not last as expected. Only 270 days.
RBR CTD-Tu	September 23, 2019	July 31, 2021	Worked as programmed
CT2X	NA	NA	Instrument failed, took water.
HOBO 20606804	February 1, 2020	November 29, 2020	Worked as programmed
HOBO20636103	February 1, 2020	November 29, 2020	Worked as programmed
HOBO20649320	February 1, 2020	November 29, 2020	Worked as programmed
HOBO20649323	February 1, 2020	November 29, 2020	Worked as programmed
HOBO20659339	February 1, 2020	November 29, 2020	Worked as programmed

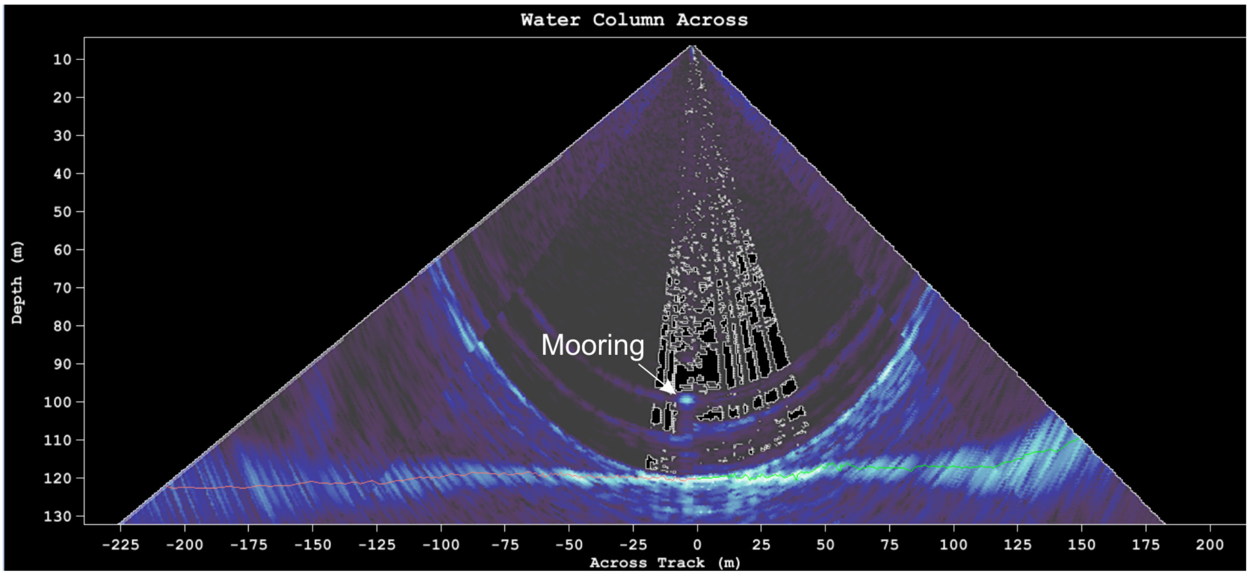

Figure 10: Mooring imaged by the EM302.

5.5 Remotely operated vehicle Comanche

The Comanche 38 ROV (Fig. 11) has two colour cameras. Its primary camera is a high-definition (HD) mini-Zeus video camera recording video with green lasers 10 cm apart, and from which frame grabs can be captured in real-time. The second camera is a high definition (HD) camera (1Cam Alpha, Sub C Imaging, 24.1 megapixels) and two green lasers 6.25 cm apart for size indication, which is also capable of capturing high-resolution still images. A third camera is used by the pilots for navigation for which videos are not recorded. Similarly, small cameras viewing the ROV umbilical cable attachment to the ROV and viewing the stern of the ROV, are visible to the pilots during operation for which videos are also not recorded. Digital still camera images can be recorded from the 1Cam Alpha, but there is not a dedicated camera for still images. This ROV also has push-corers for the targeted collection of sediment samples, which were used during the Scott Inlet dive.

Figure 11: The Comanche ROV being deployed at Southwind Fjord. Photograph by A. Normandeau. NRCan photo 2021-262.

Two dives were specifically dedicated to geological research and of which all seafloor imagery are archived at the Geological Survey of Canada and Fisheries and Oceans Canada. However, many other dives were completed as part of a NSERC STAC-funded project to survey deep-water coral and seep habitats in Northern Labrador and Baffin Bay. The first strictly geological dive (station 15, dive no 22) was completed in Southwind Fjord to image an iceberg-triggered submarine landslide. The dive mainly consisted of upslope transects at different locations to image the geomorphological variability of the depositional and erosional zones of the landslide, as well as the headscarp and iceberg pits.

The second strictly geological dive dive (station 26, dive no 27) targeted submarine channels on the margin of Scott Trough where multibeam bathymetry indicated the presence of sediment waves that could be formed by slope instability related to the current hydrocarbon seep activity (Cramm et al., 2021). The ROV survey of this site began in the depositional area of the turbidity current channels, characterized by the sediment waves. Using the USBL feed from the ROV overlaid onto the high-resolution multibeam sonar map of the site to determine sample locations in real-time, three ROV push-cores were collected from the stoss and lee sides of the sediment waves to assess the depth of muddy sediment over the top of the sandy bedforms. The push-cores did not have core catchers, and some of the sandy sediment comprising the sediment waves themselves was lost from the bottom of the core. A few centimetres of sandy sediment were nonetheless preserved in the push cores and will be used to assess the age of the last turbidity current to flow in the area.

REFERENCES

Bennett R, Campbell DC, Furze MFA. 2014. The shallow stratigraphy and geohazards of the Northeast Baffin Shelf and Lancaster Sound. Bulletin of Canadian Petroleum Geology **62** : 217–231. DOI: 10.2113/gscpgbull.62.4.217

Broom LM, Campbell DC, Gosse JC. 2017. Investigation of a Holocene marine sedimentary record from Pond Inlet, northern Baffin Island, Nunavut. Canada-Nunavut Geoscience Office, Summary of Activities 2016 : 93–104.

Cramm MA, de Moura Neves B, Manning CCM, Oldenburg TBP, Archambault P, Chakraborty A, Cyr-Parent A, Edinger EN, Jaggi A, Mort A. 2021. Characterization of marine microbial communities around an Arctic seabed hydrocarbon seep at Scott Inlet, Baffin Bay. Science of The Total Environment **762** : 143961.

Edinger E, de Moura Neves B., Belanger D, Wareham-Hayes VE, Sherwood O, Campbell DC. 2017. Arctic bamboo coral forests as millennium-scale ecosystem engineers. 121 pp.

Ghienne J, Normandeau A, Dietrich P, Bouysson M, Lajeunesse P, Schuster M. 2021. The depositional signature of cyclic steps: A late Quaternary analogue compared to modern active delta slopes. Sedimentology **68** : 1502–1538.

Gosse JC, Tremblay T, Broom LA, Campbell DC, Wenzel G, Nedimoviæ MR, Brisson LF. 2020. Initial results from the ULINNIQ seismicity and tsunami hazard project , northeastern Baffin Island , Nunavut. Canada-Nunavut Geoscience Office, Summary of Activities 2019 : 101–124.

Higman B et al. 2018. The 2015 landslide and tsunami in Taan Fiord , Alaska. Scientific Reports **8** : 12993. DOI: 10.1038/s41598-018-30475-w

Hughes-Clarke JE, Muggah J, Renoud W, Bell T, Forbes DL, Cowan B, Kennedy J. 2015. Reconnaissance seabed mapping around Hall and Cumberland peninsulas, Nunavut : opening up southeastern Baffin Island to nearshore geological investigations. Canada-Nunavut Geoscience Office, Summary of Activities 2014 : 133–144.

Jenner KA, Campbell DC, Piper DJW. 2018. Along-slope variations in sediment lithofacies and depositional processes since the Last Glacial Maximum on the northeast Baffin margin , Canada. Marine Geology **405** : 92–107. DOI: 10.1016/j.margeo.2018.07.012

Kostylev VE, Broom LM, Robertson AG, Carson TE, Hayward SE, Kostylev VE, Broom LM, Robertson AG, Carson TE, Hayward SE. 2020. CCGS Amundsen 2020804 expedition : seabed habitats and marine geohazards in the Northeast Newfoundland Slope , Labrador Sea OPEN FILE 8749 CCGS Amundsen 2020804 expedition : seabed habitats and marine. Geological Survey of Canada Open File **8749**

de Moura Neves B, Edinger E, Hillaire-Marcel C, Saucier EH, France SC, Treble MA, Wareham VE. 2015. Deep-water bamboo coral forests in a muddy Arctic environment. Marine Biodiversity **45** : 867–871.

Mudie PJ, Piper DJW, Rideout K, Robertson KR, Schafer CT, Vilks G, Hardy IA. 1984. Standard Methods For Collecting, Describing and Sampling Quaternary Sediments At the Atlantic Geoscience Center. Geological Survey of Canada Open File **1044** : 47.

Normandeau A et al. 2018. CCGS Hudson Expedition 2018042: Marine geohazards and natural seeps off southeastern Baffin Island. Geological Survey of Canada Open File **8488** : 1–91. DOI: 10.4095/xxxxxxx

Normandeau A, Campbell DC, Bennett R, Macquarrie M, Mackillop K, Philibert G, Sedore P, Maselli V, Jenner KA. 2020. Holocene and active marine geohazards offshore eastern Baffin Island, Nunavut. Canada-Nunavut Geoscience Office, Summary of Activities 2019 : 93–100.

Normandeau A, Dietrich P, Clarke JH. 2019a. Retreat Pattern of Glaciers Controls the Occurrence of Turbidity Currents on High - Latitude Fjord Deltas (Eastern Ba fin Island). Journal of Geophysical Research: Earth Surface **124** : 1–13.

Normandeau A, Mackillop K, Macquarrie M, Philibert G, Bennett R. 2021a. Southwind Fiord, Baffin Island, Nunavut : a natural laboratory to explore modern turbidity currents, submarine landslides and iceberg scouring in an Arctic environment. Canada-Nunavut Geoscience Office, Summary of Activities 2020 : 81–92.

Normandeau A, Mackillop K, Macquarrie M, Richards C, Bourgault D, Campbell DC, Maselli V, Philibert G, Clarke JH. 2021b. Submarine landslides triggered by iceberg collision with the seafloor. Nature Geoscience **14** : 599–605. DOI: 10.1038/s41561-021-00767-4

Normandeau A, Robertson A, Philibert G, Regular K, Sedore P, Normandeau A, Robertson A, Philibert G, Regular K, Sedore P. 2019b. R/V Nuliajuk expedition 2019Nuliajuk : Marine geohazards near Qikiqtarjuaq, Padle Fjord, Southwind Fjord and Pangnirtung, Southeast Baffin Island (Nunavut). Geological Survey of Canada Open File **8641**

APPENDIX A: STATION SUMMARY

Table A5: Summary of all stations

2021805 Core Summary

Vessel: CCGS Amundsen | **Date: July 15 - August 12, 2021**

Station No.	Sample Type	AMD -ID	Day / Time (UTC)	Latitude	Longitude	Location	Water Depth (m)	Corer length (cm)	App. Penetration (cm)	Core length (cm)	No. of Sections	Bagged	Comments
001	GGC	Makkovik	201/20:21:18	55.5447	-58.88081	Makkovik	779	900	900	578	4	Y	
002	BC	-i-8.5a	203/09:24:36	56.59853	-60.81166	-in - inner	130			A:21 / B:25	1	N	Surface washed by water
003	PC	-i-8.5a	203/10:37:24	56.59853	-60.81166	-in - inner	133.5	900	600	488	4	N	TWC = Empty / Core top is soupy and was settled for 30 min.
004	BC	-i-8.5b	203/14:44:21	56.69322	-60.28469	-in - outer	473			A:38 / B:39.5			1 mm of misxing during box transport. Water preserved at surface. Lots of biodivesity. No to negligeable compaction during push coring
005	PC	-i-8.5b	203/15:55:41	56.69294	-60.2851	-in - outer	473	900	900	542.5	4	Y	TWC = 113 cm
006	BC	Hatton Sill	208/ 07:43:41	61.4421	-60.56568	Hatton Sill	895			A: 38 / B:27 / C:28.5 / D:38.5 / E:28.5 / F:32			A wasn't compressed, all others were. 20cm diameter Geodia sponge. Abundant sponge mats throughout. Abundant bamboo coral fragments ans scallop shells
007	GGC	Hatton Sill	208/19:06:20	61.439	-60.57431	Hatton Sill	972	900	150	120	1	N	
008	BC	Hatton Sill	208/20:11:29	61.44488	-60.56928	Hatton Sill	924			A:32.5 / B:34			1/2 to 1/3 full washed on side. 2 push cores down full side. Sponge mat around with at least 3 different sponges on surface.
009	GGC	Hatton Sill	208/21:24:04	61.44488	-60.57025	Hatton Sill	860	900	300	196	2	N	
010	BC	Davis Strait	209/22:19:23	63.4016	-58.53774	Davis Strait	1080			A:34.5 / B:32.5 / C:35.5 / D:34.5			Minor compaction.
011	GC	Davis Strait	210/08:31:36	63.34838	-58.25756	Davis Strait	1280	300		120	1	N	
012	GGC	Davis Strait	210/22:22:11	63.34666	-58.20126	Davis Strait	1296	900	300	217	2	N	Section between AB and BC flowed out but was retained. Sed. Struct. Might be affected

013	GC	Davis Strait	210/23:42 :00	63.347 1	- 58.203 35	Davis Strait	1297	300		0	0	Y	Small section bagged. No core liner
014	Moor ing	SF-3.1	212/11:29	66.761 698	- 62.339 844	Southwind Fjord	120	-	-	-	-	-	Tried connecting. Failed 5 times. Changed position. Connected the second time. Ranged at 360m.Decided to release since we were communicating
015	ROV	SF-ROV / Dive C0022	212/13:38	66.751 8	- 62.313 969	Southwind Fjord	50	-	-	-	-	-	Deployment at 13:38. Bottom at 13:57. Recovery at 15:46. 2 transects along the headscarp. 3 transects upslope.
016	BC	SF-6.2a	212/17:08	66.751 27	- 62.312 35	Southwind Fjord	38	-	-	A:29 / B:26	-	-	In 2018 landslide glide plane
017	BC	SF-6.2b	212/17:26	66.752 58	- 62.311 58	Southwind Fjord	38	-	-	A:26	-	-	Outside of 2018 landslide
018	CTD	SF-3.1	212/18:43	66.760 79	- 62.334 08	Southwind Fjord	120	-	-	-	-	-	
019	PC	SF-6.1	212/23:22 :54	67.025 69	- 62.580 44	Padloping Through	805	900	600-900	659.5	5	N	TWC = 120cm. Piston split at 50cm. Piston rubber was not tighten too much.
020	BC	Disko Fan	214/02:20 :39	67.882 32	- 59.382 27	Disko Fan	950			38.5			Laura's core
021	PC	Disko Fan	214/22:56 :23	67.968 24	- 59.489 85	Disko Fan	868	900	300	44	1	N	TWC=39 cm
022	GC	Disko Fan	215/00:02 :39	67.969 3	- 59.494 56	Disko Fan	878	300		45		N	
023	PC	Scott Inlet-Deep	217/22:25 :30	71.396 29	- 70.313 16	Scott Inlet	700	900	300	253			No TWC. Core triggered too early. Wired back up a bit and went back down into the sediment a second time. Caution while a-lysing.
024	BC	Scott Inlet-Deep	217/23:34 :09	71.396 12	- 70.312 52	Scott Inlet	700			A: 41 / B:41 / C:37.5 / D:36 / E:38.5			No compression on A and B. Compression of 2cm on the other push cores.
025	PC	Scott Inlet-Deep	218/00:51 :00	71.396 2	- 70.312 83	Scott Inlet	700	900	300	194			TWC=74cm
026	ROV	Scott Inlet ROV 4	218/17:57 :01	71.339 12	- 70.260 52	Scott Inlet	400- 200						ROV dive on submarine turbidite channel going upslope to an iceberg-scoured shelf. 3 push cores (035,. 036, 037). Red/green = A, Red Yellow, Green = B, Green, Yellow/Red = C. Colors from bottom to top.
027	PC	Scott Inlet Piston Core 3	218/22:00 :02	71.397 66	- 70.315 66	Scott Inlet	697.9 5	900	300	0			Bagged

028	BC	Scott Inlet Box Core 2	219/01:07:42	71.33953	-70.25831	Scott Inlet	377.48			A:19 / B:19 / C:18 / D:17			
029	GGC	Gib-3.1	219/14:26:00	70.64923	-72.47546	Gibbs Fjord	302	900	900	448.5	3	Y	
030	GGC	Gib-3.2	219/17:31:04	70.804	-72.20167	Gibbs Fjord	261	900	300	181	2	N	
031	GGC	Cla-3.1	219/19:23:39	70.88742	-72.28746	Clark Fjord	267	900	150	89.5	1	N	
032	BC	Cla-3.2	219/20:38:42	70.92842	-72.30155	Clark Fjord	207			A:10.5 / B:12			
033	BC	Cla-3.1	219/21:17:46	70.88492	-72.29695	Clark Fjord	260			A:30.5 / B:30.5			
034	GGC	Pangnirtung Piston Core	222/14:00:30	66.16406	-65.72013	Pangnirtung Fjord	150.24	900	450	277	2	Y	
035	Push	26A	218/ 18:45:56	71.33924	-70.25766	Scott Inlet	376.8			15			Core tube is green/red tape
036	Push	26B	218/ 18:53:43	71.33891	-70.25697	Scott Inlet	368.1			20			Core tube is Red - Yellow - Green
037	Push	26C	218/ 19:02:59	71.33883	-70.25679	Scott Inlet	368.2			13			Core tube is Green – Yellow - Red

2021806 Core Summary

Vessel: CCGS Amundsen **Date: July 15 - August 12, 2021**

001	PC	Leg3_01	234/17:12	67.27927	-62.21981	Merchant	413.56	900	700	450	3	Y	
002	BC	Leg3_02.1	238/13:25	67.72733	-63.34261	Broughton	582.8			38			1cm compaction
003	GGC	Leg3_02.2	238/14:07	67.72835	-63.34318	Broughton	585	300	300	279	2		Rond + Alex.N : A-B = 1.50m C-D + 1m29
004	PC	Leg3_03	238/18:13	67.60011	-63.60388	Broughton	595	900	900	500	4	Y	TWC: 49 cm

APPENDIX B: GEOGRAPHIC LOCATIONS OF STATIONS

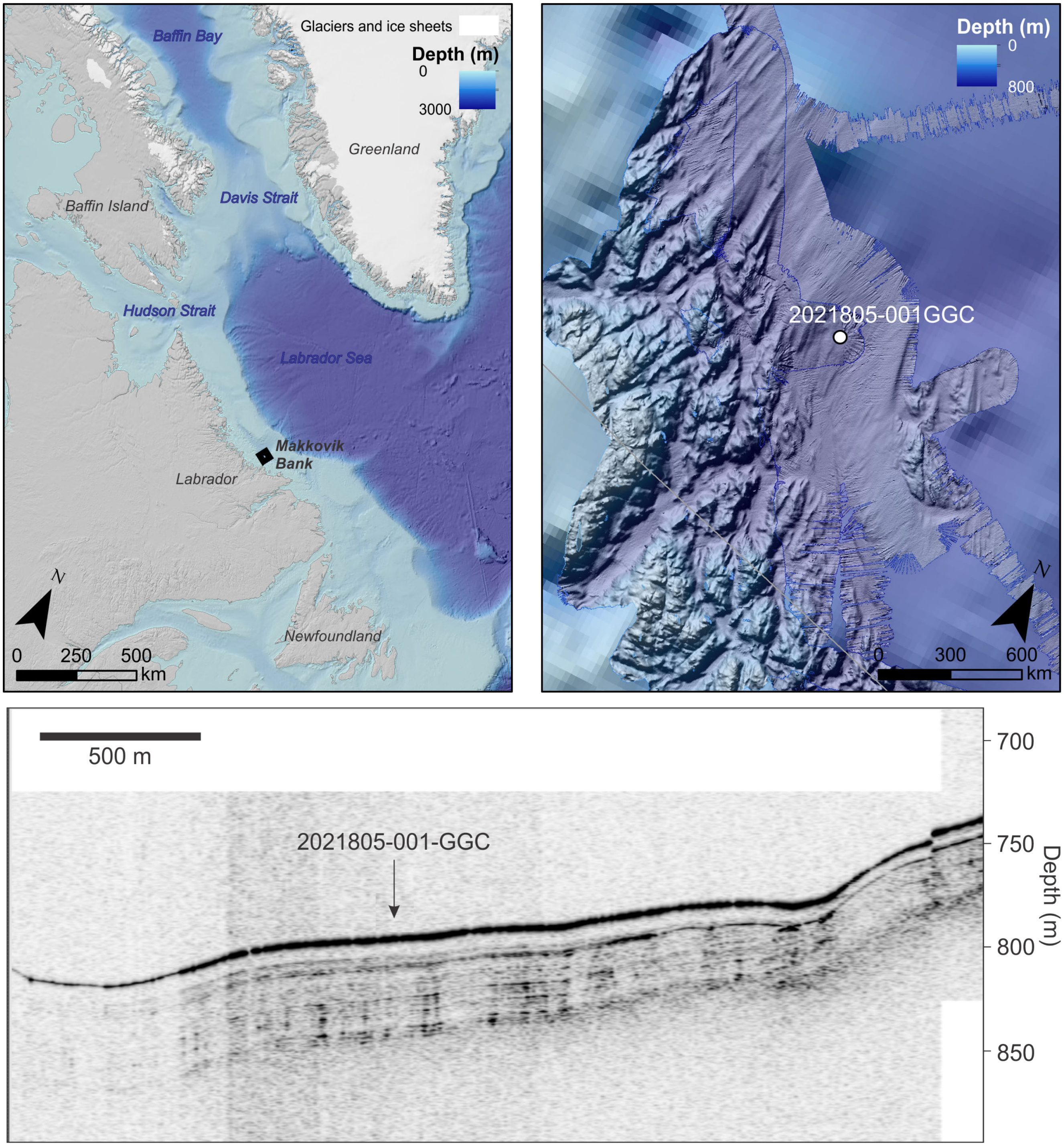

Figure B12: Location of core 2021805-001GGC on Makkovik Bank

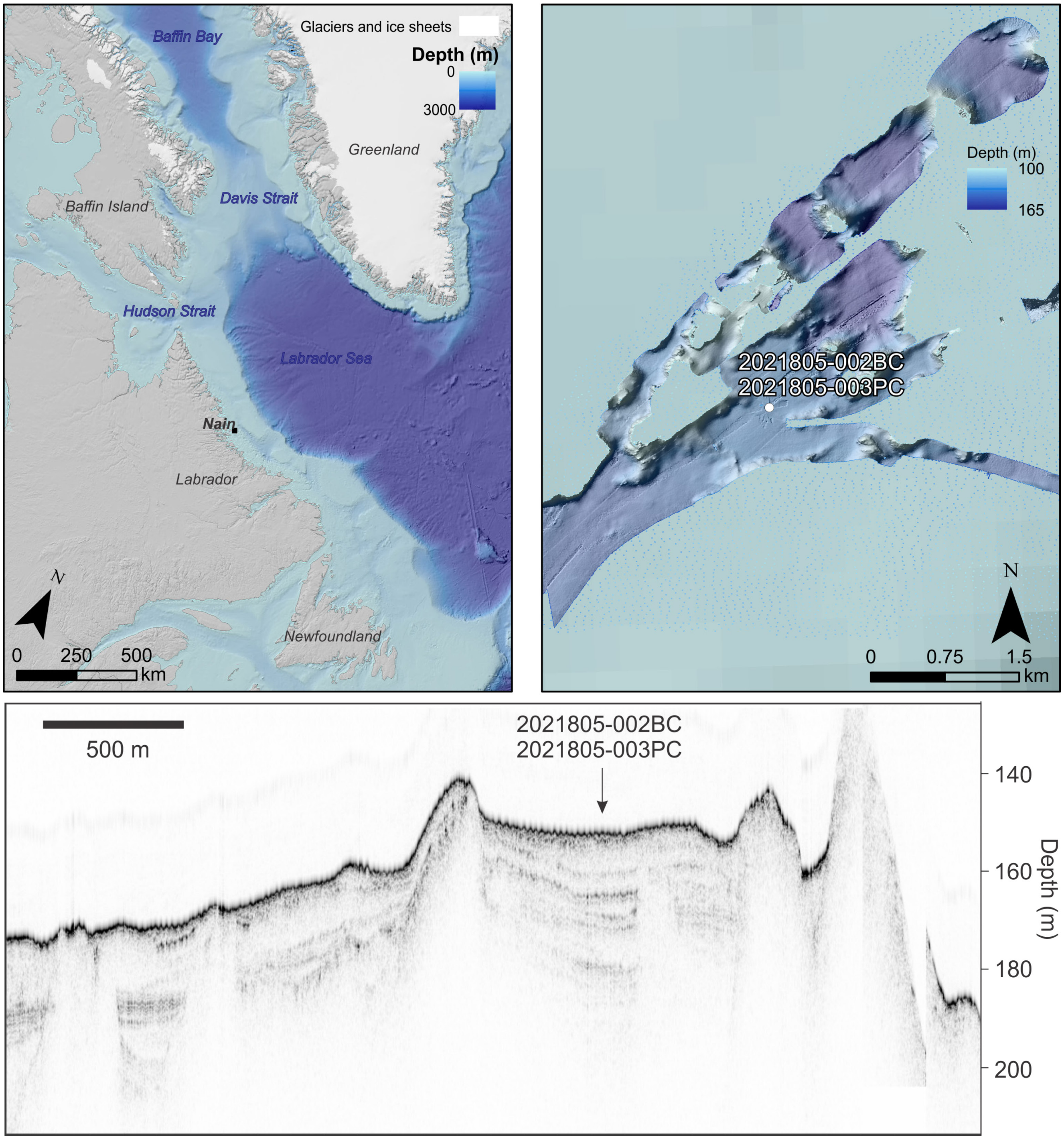

Figure B13: Location of cores 2021805-002BC and 003PC in Nain

.

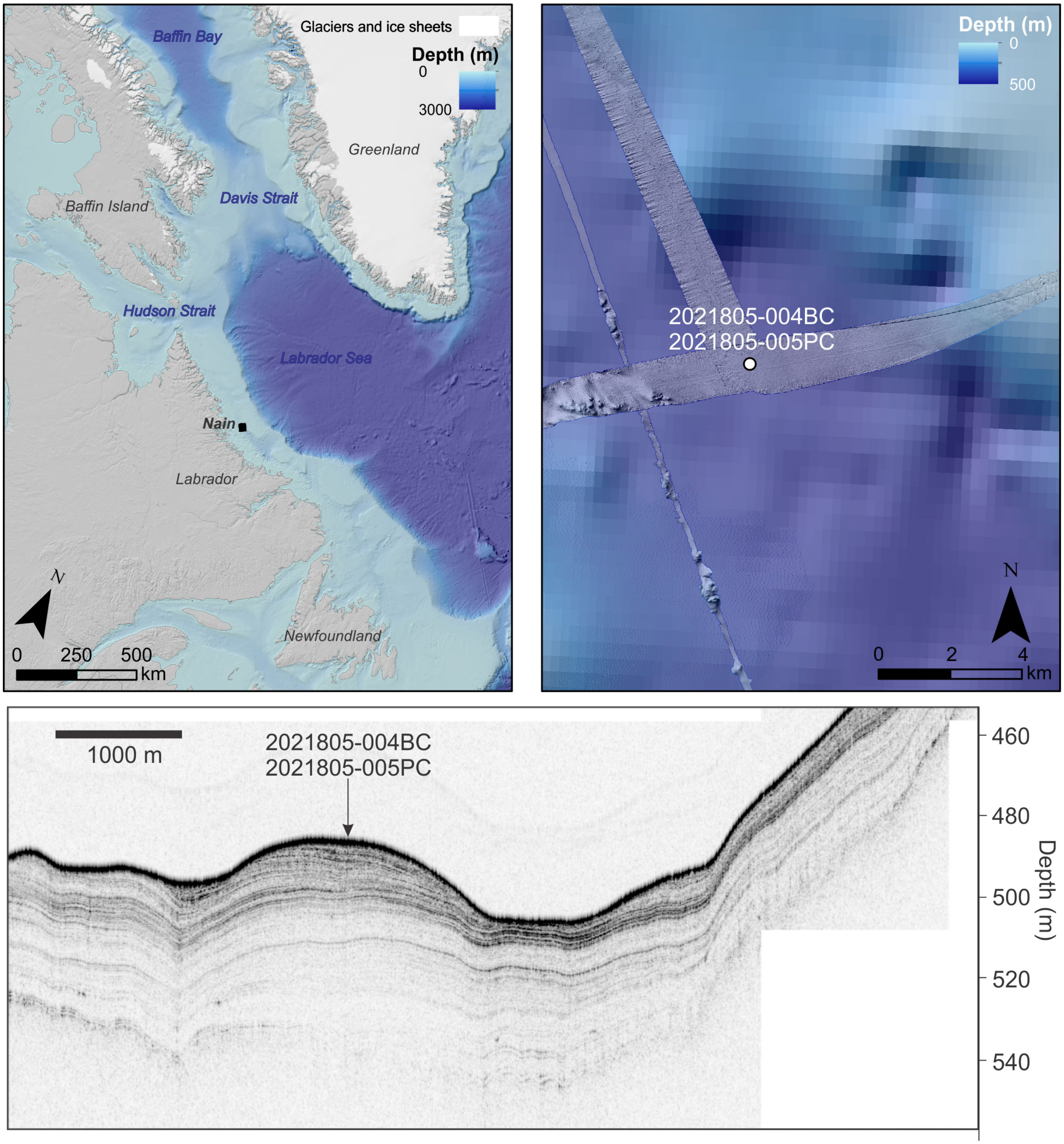

Figure B14: Location of cores 2021805-004BC and 005PC in Nain

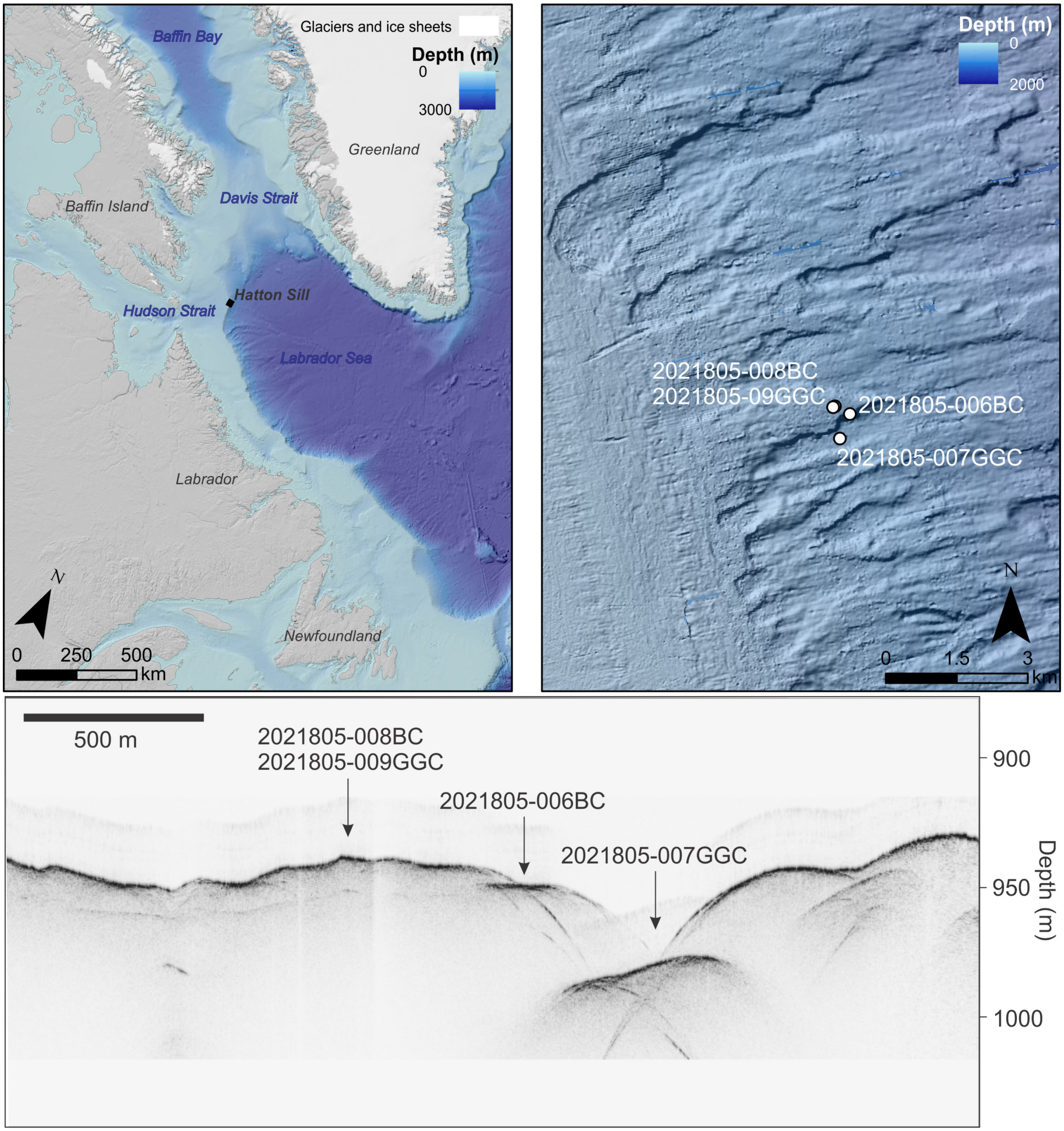

Figure B15: Location of cores 2021805-006BC, 007GGC, 008BC, 009GGC on Hatton Sill

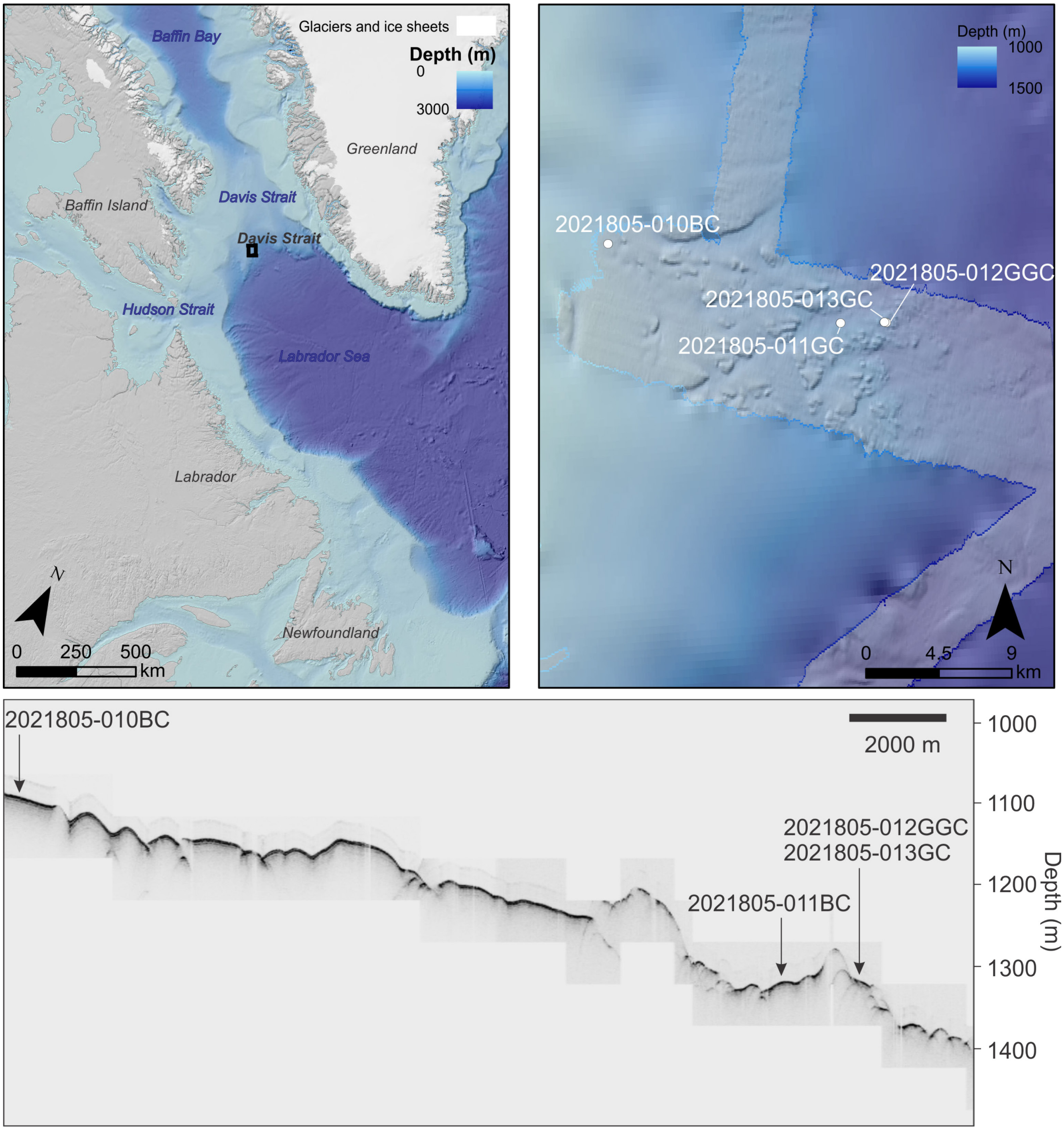

Figure B16: Location of cores 2021805-011BC, 012GGC and 013GC in Davis Strait

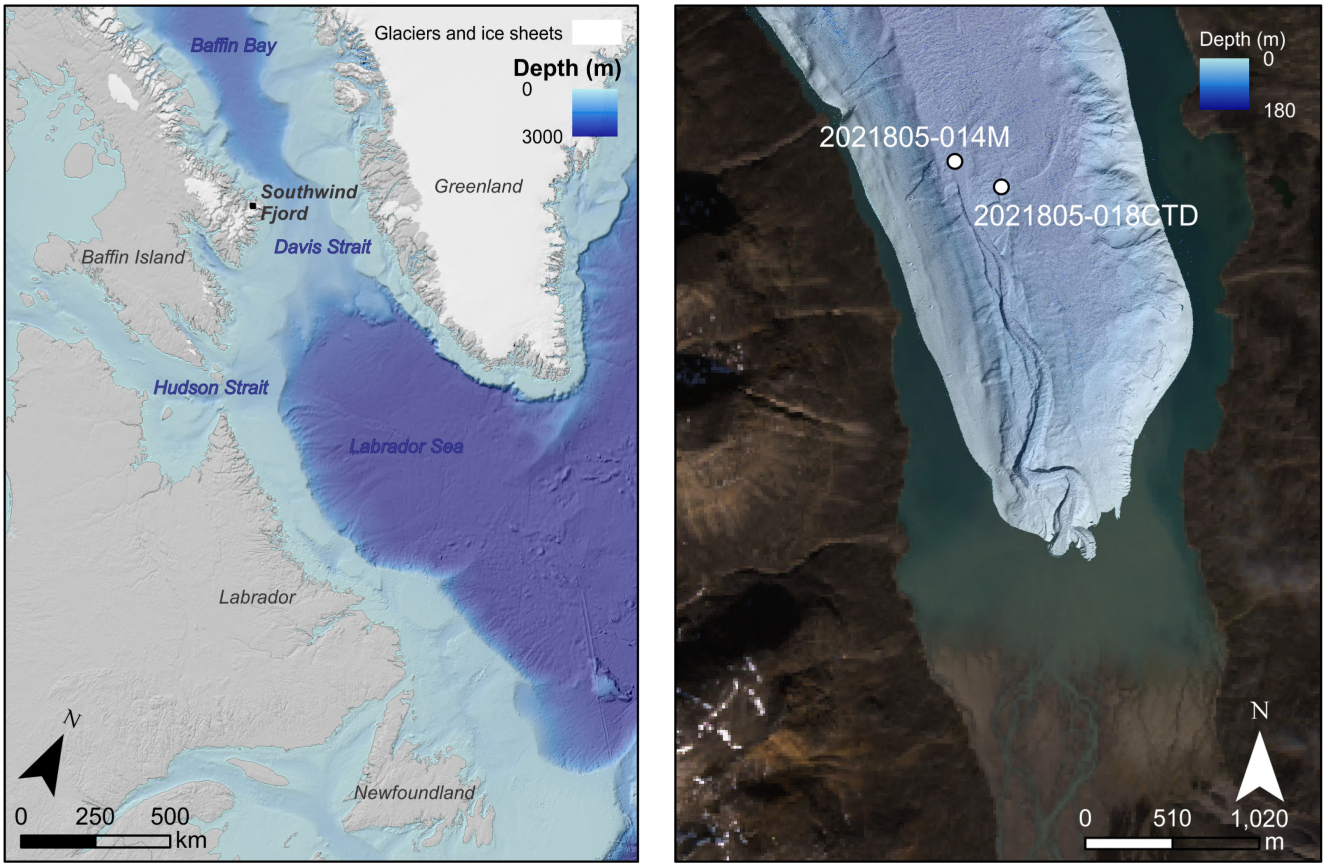

Figure B17: Location of mooring recovery station 2021805-014M and CTD profile station 0018CTD in Southwind Fjord

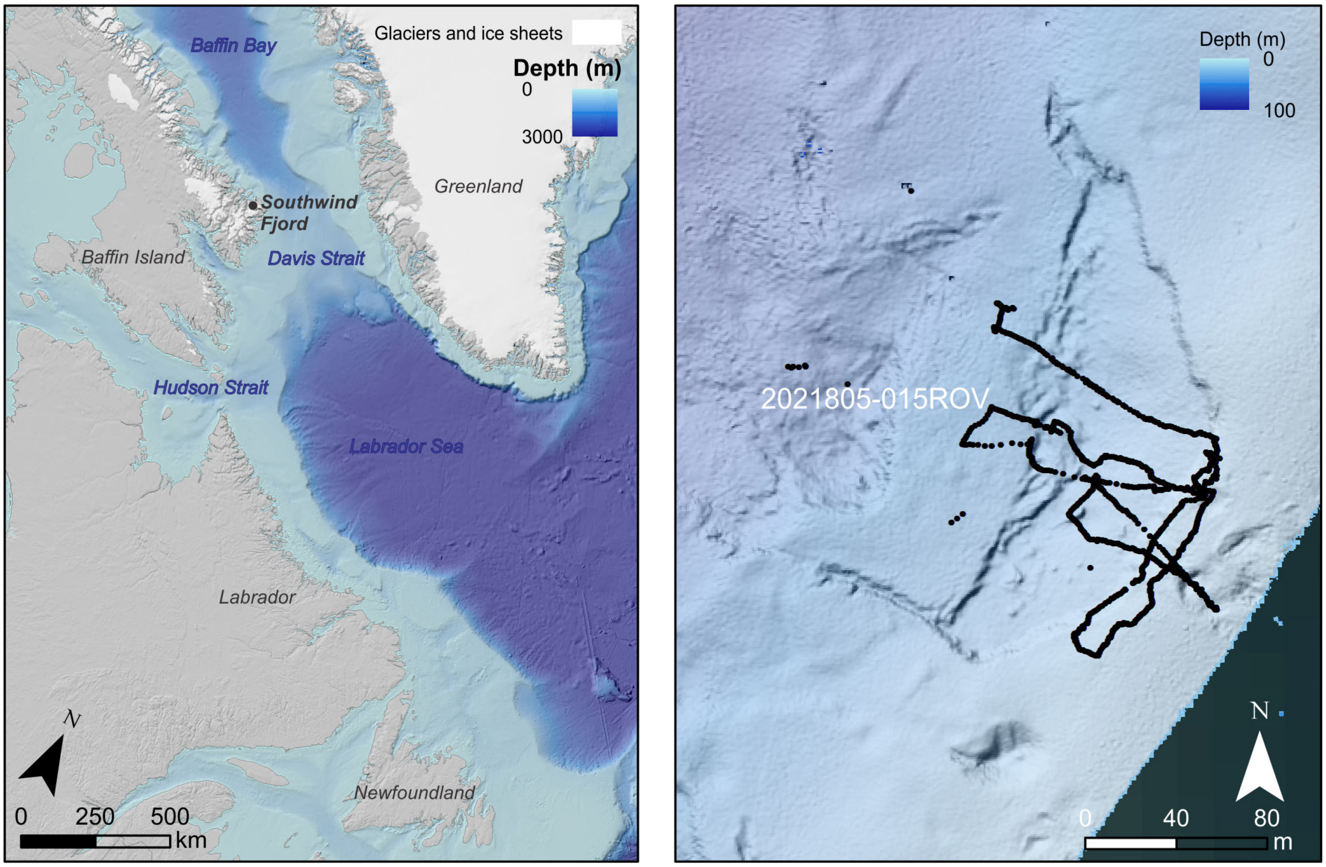

Figure B18: Location of ROV dive station 2021805-015ROV in Southwind Fjord

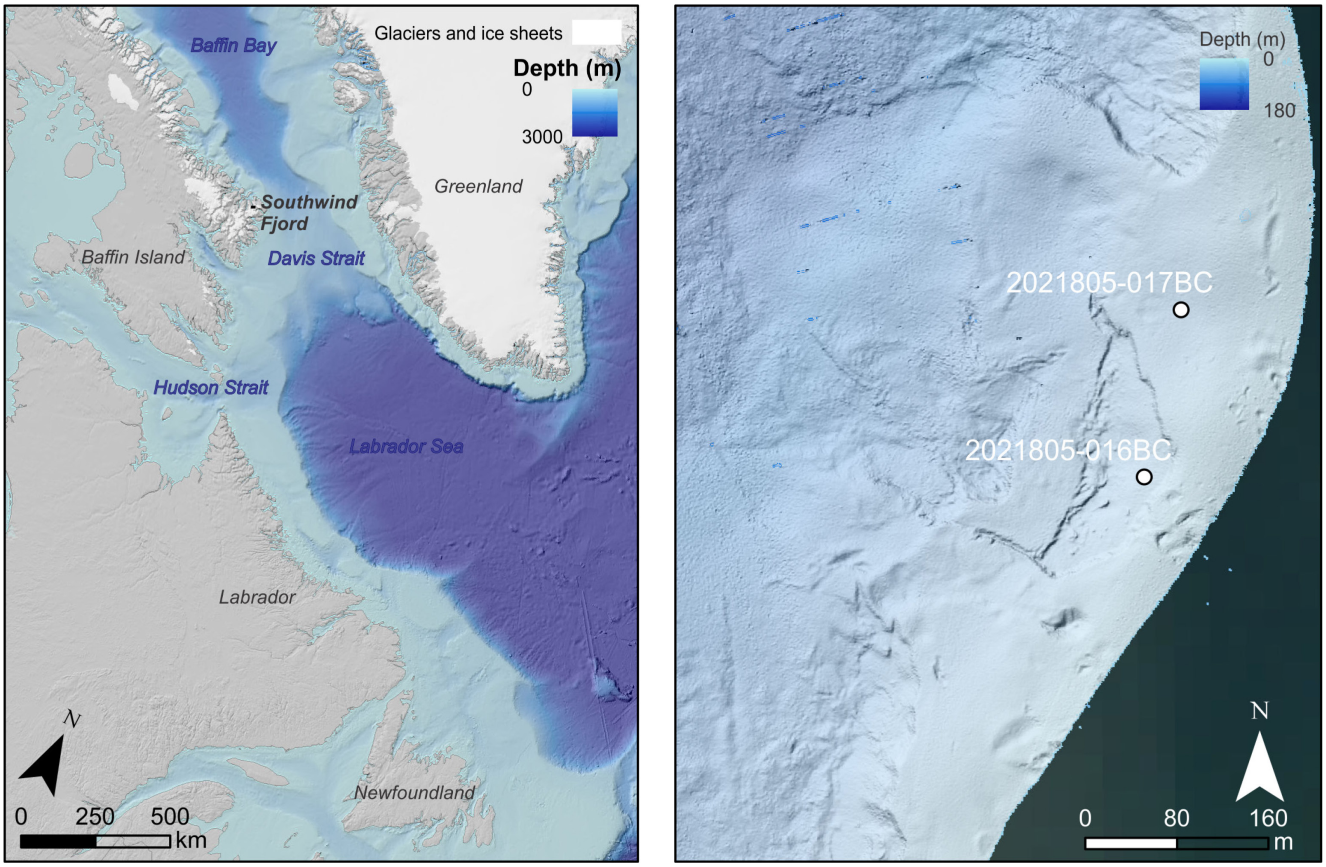

Figure B19: Location of cores 2021805-016BC and 017BC in Southwind Fjord

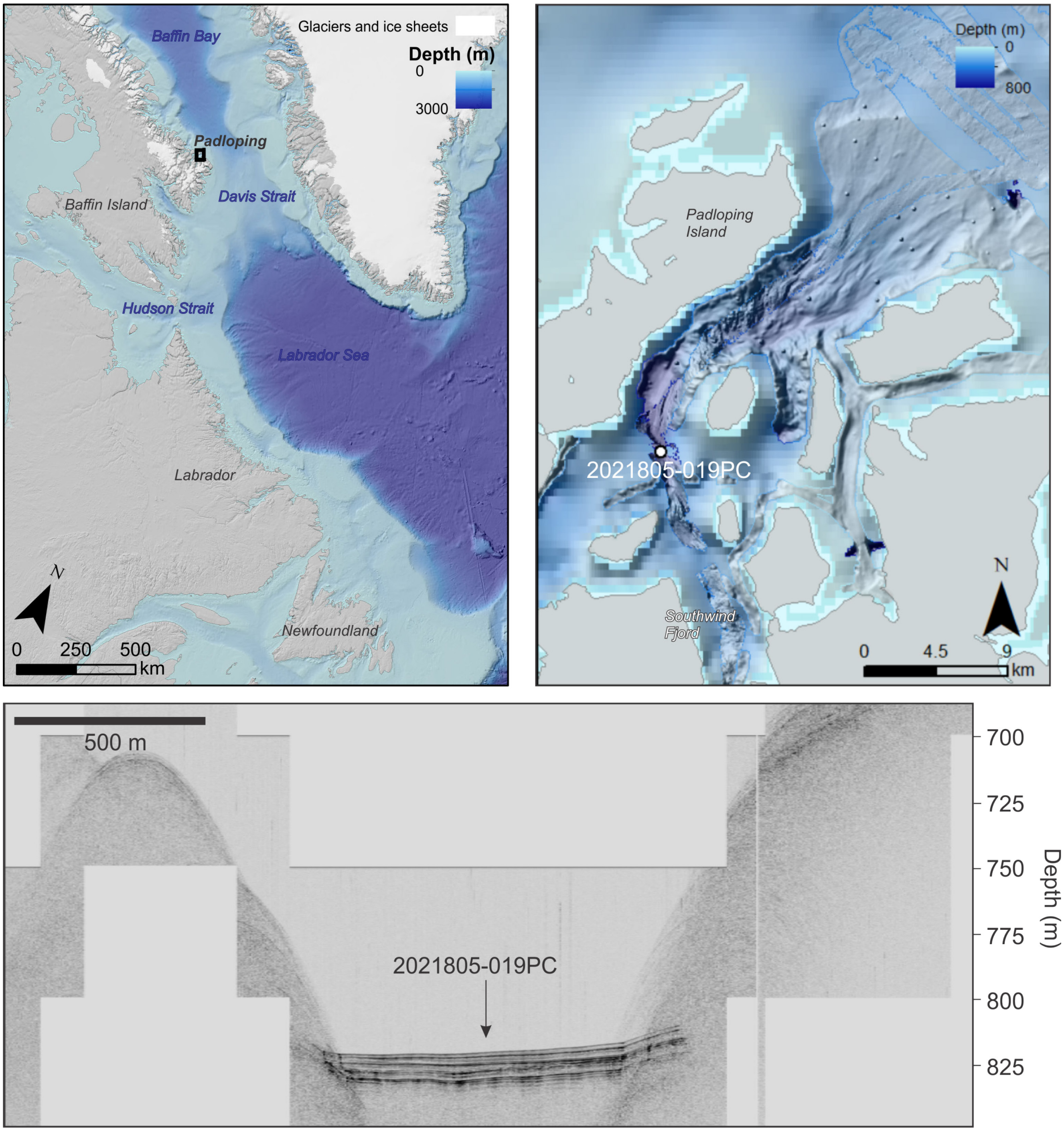

Figure B20: Location of cores 2021805-019PC in Padloping Trough

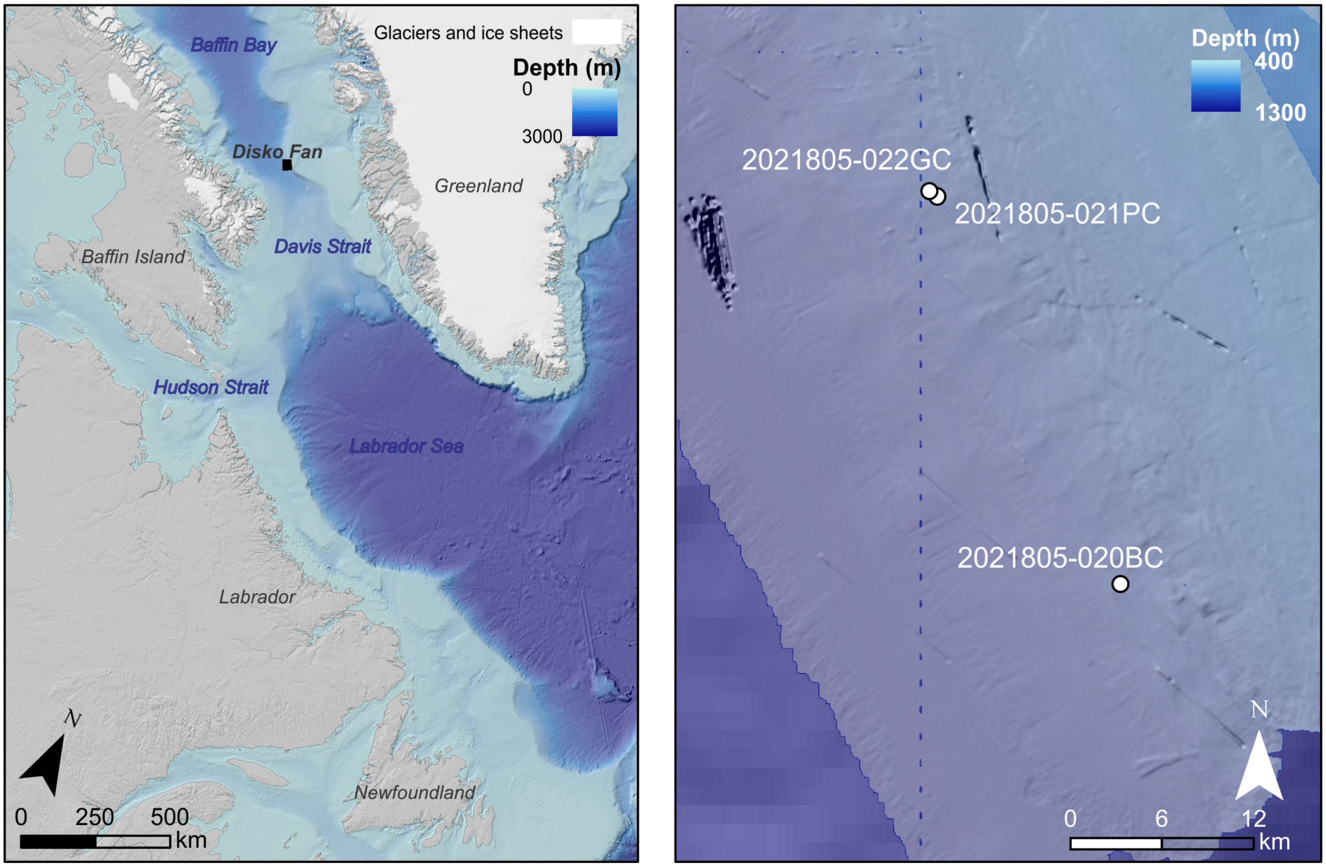

Figure B21: Location of cores 2021805-020BC, 021PC and 022GC on Disko Fan

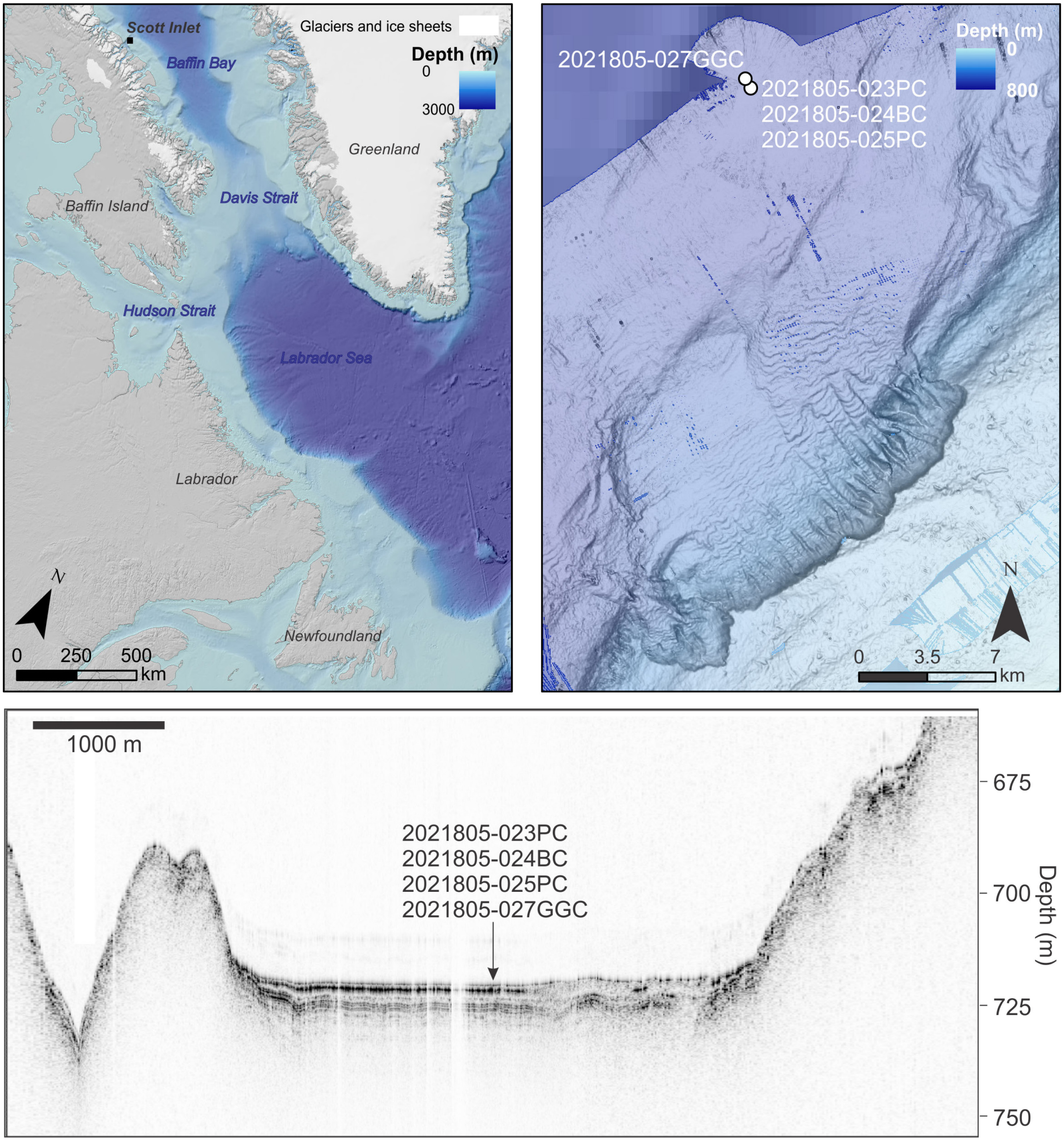

Figure B22: Location of cores 2021805-023PC, 024BC, 025PC, and 027GGC in Scott Inlet

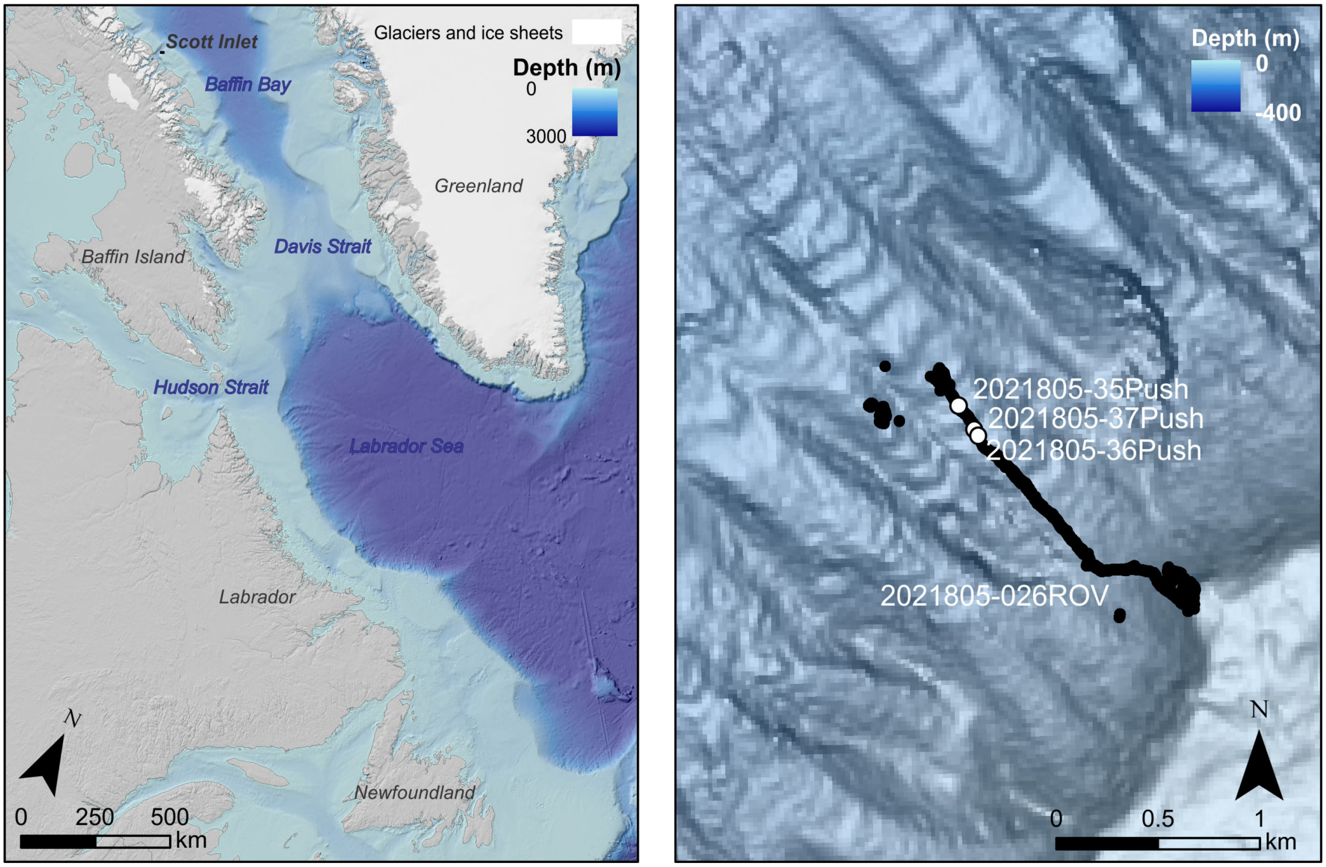

Figure B23: Location of ROV dive 2021805-026 and push cores.

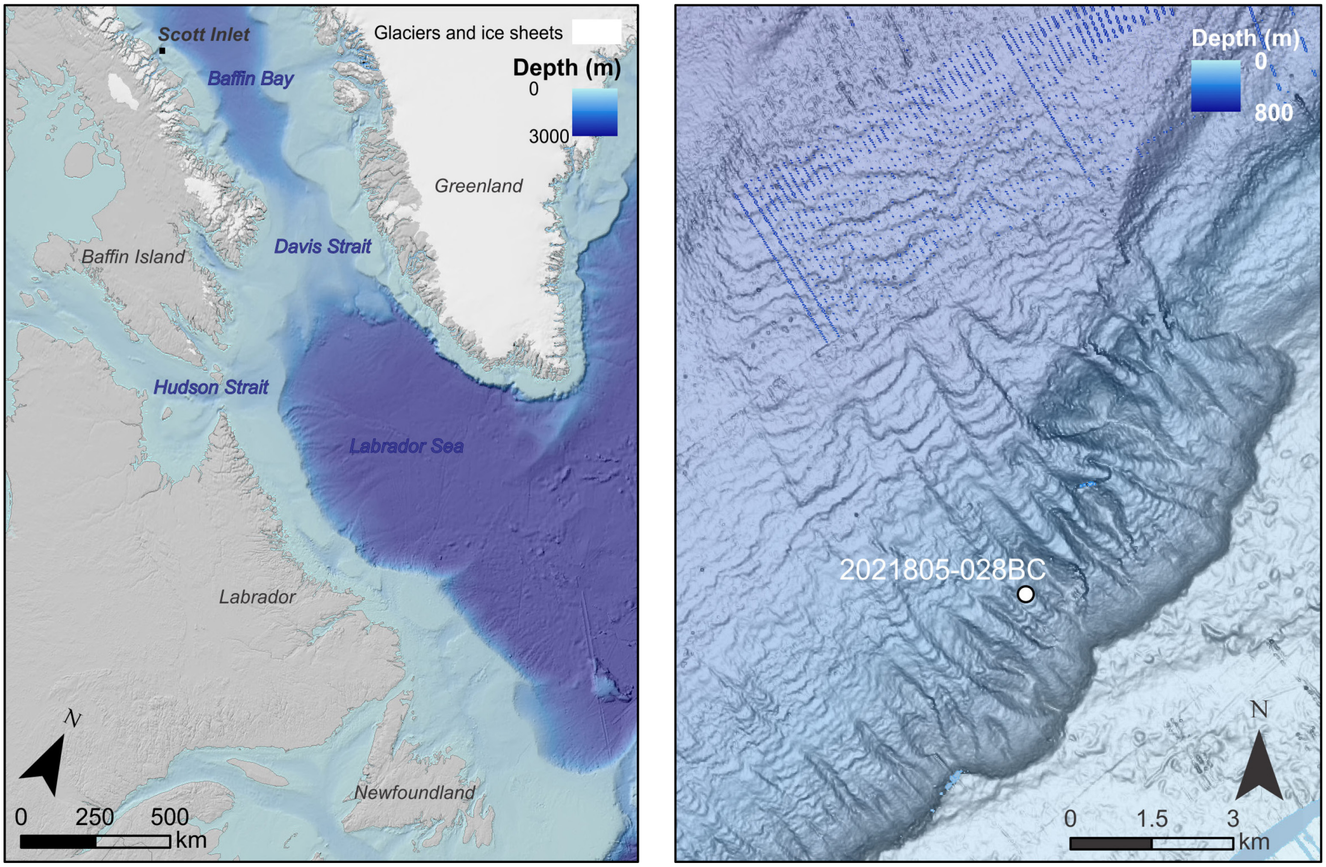

Figure B24: Location of core 2021805-028BC in Scott Inlet

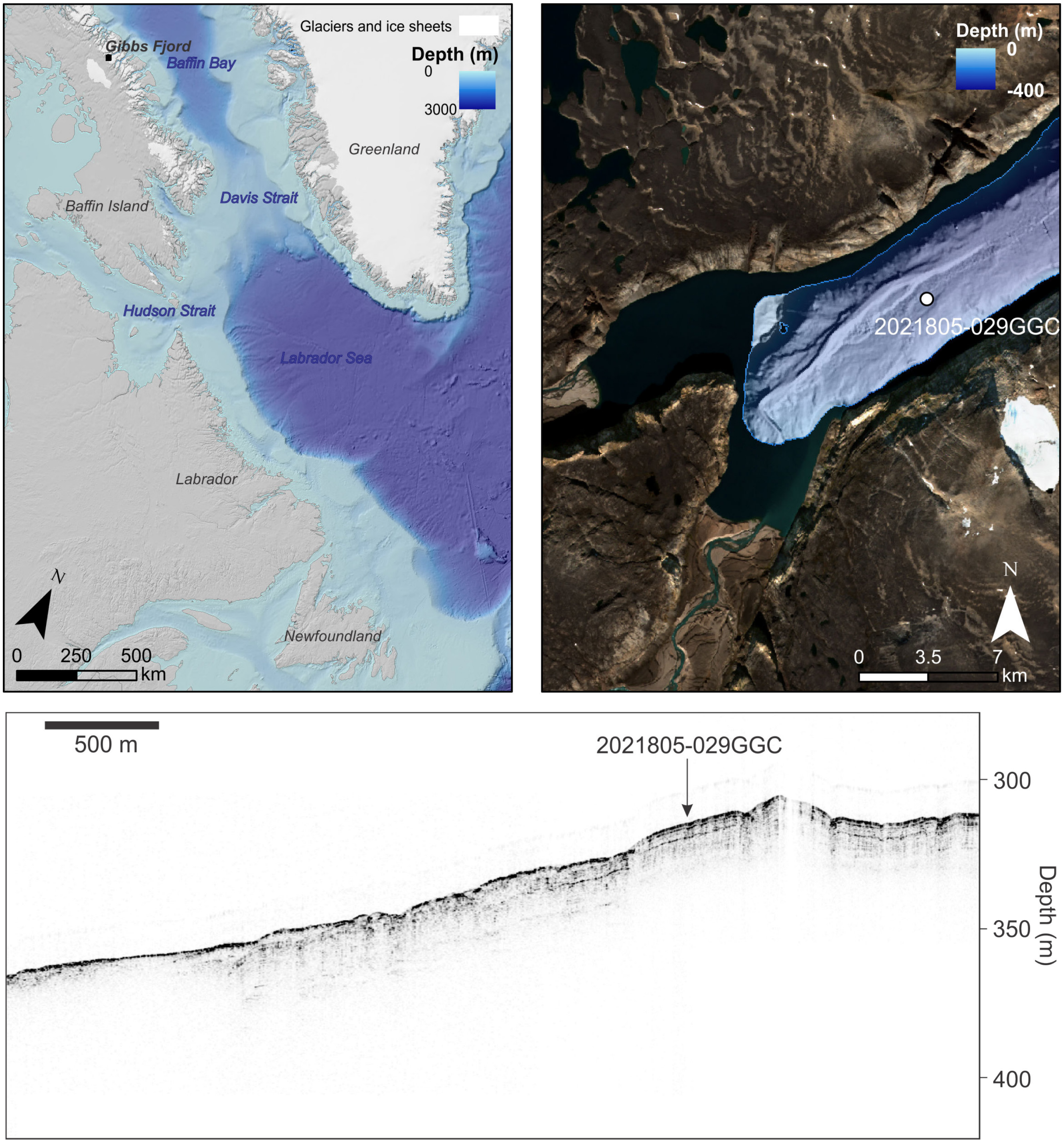

Figure B25: Location of core 2021805-029GGC in Gibbs Fjord

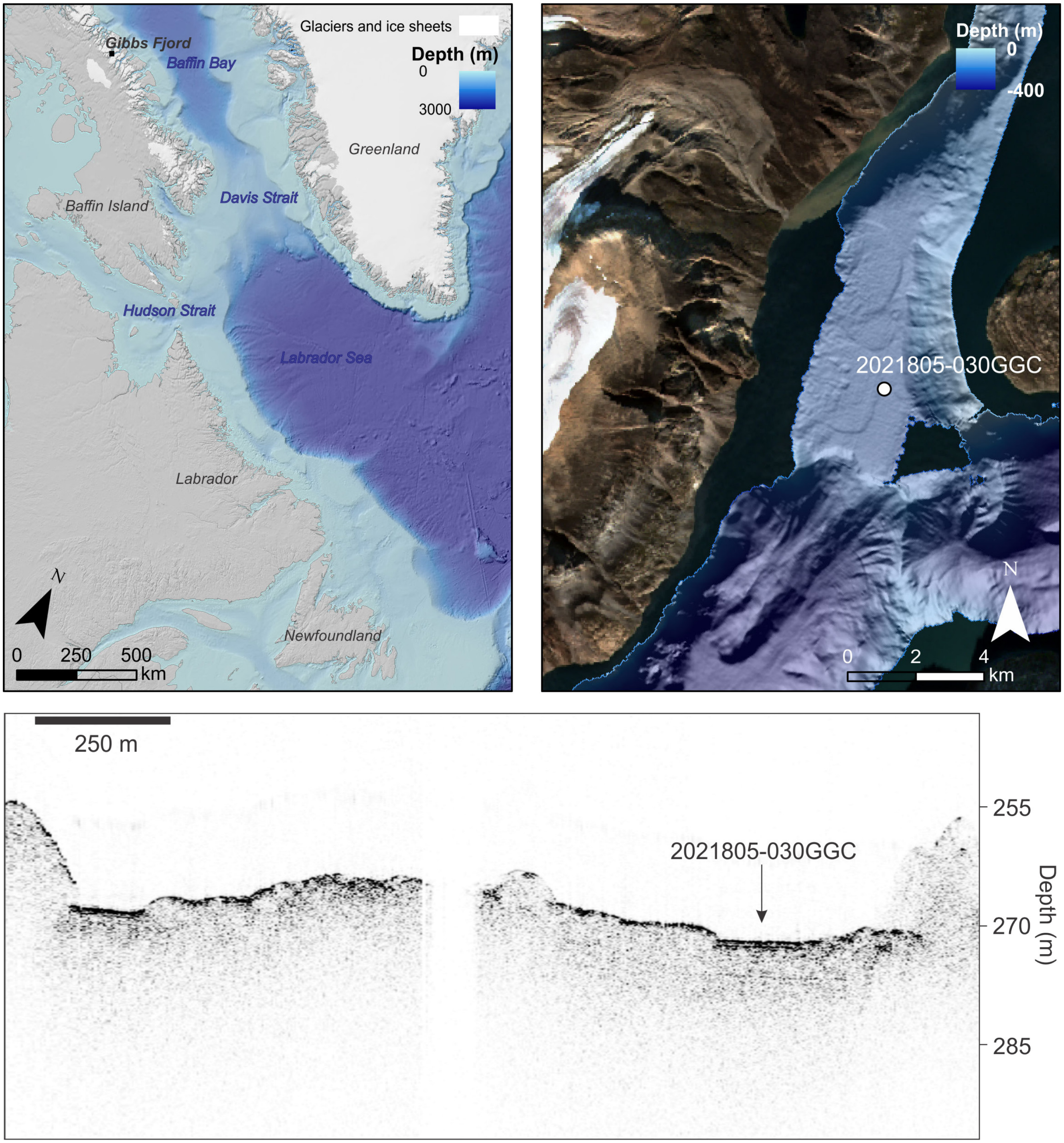

Figure B26: Location of core 2021805-030GGC in Gibbs Fjord

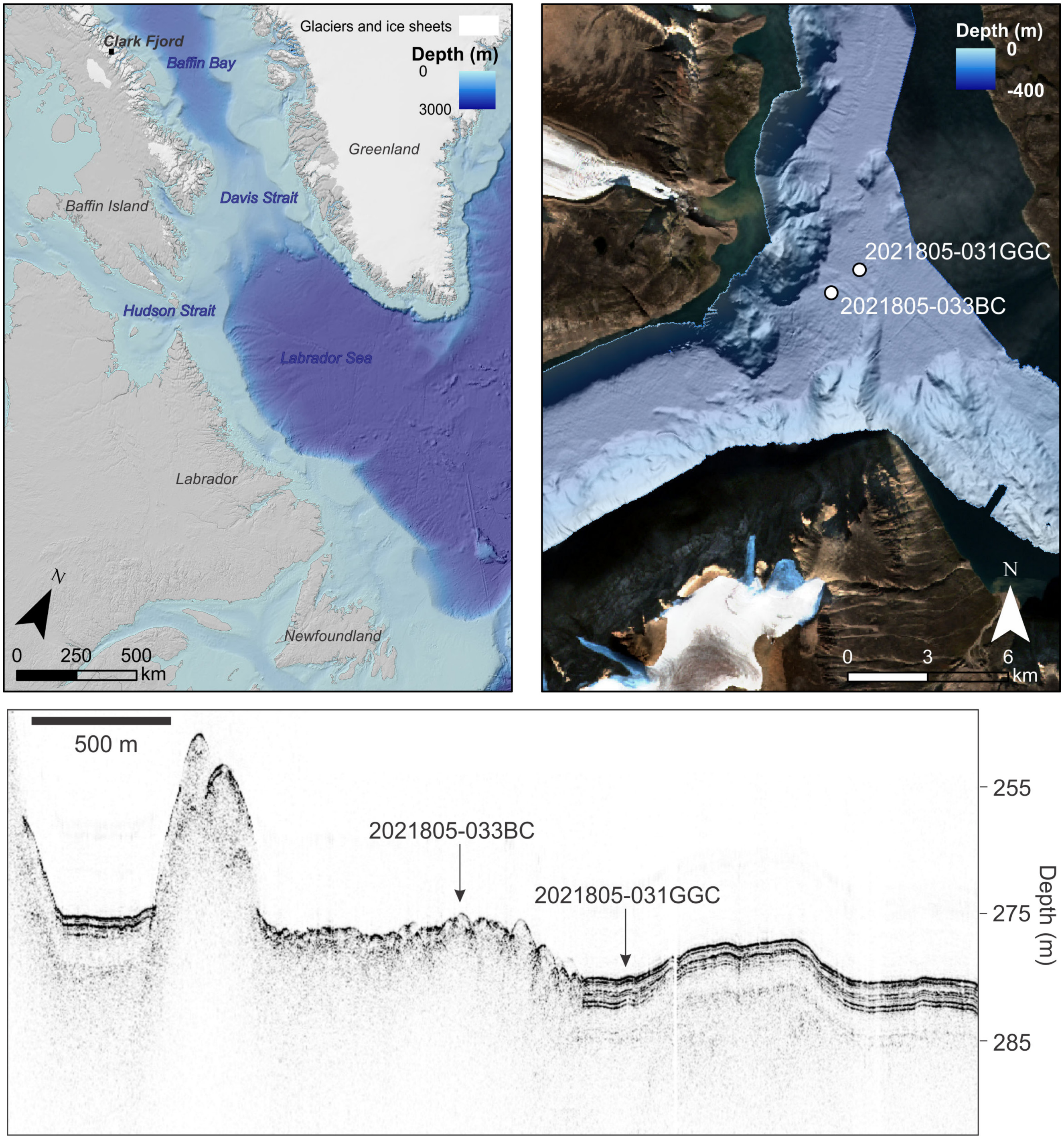

Figure B27: Location of core 2021805-031GGC and 033BC in Clark Fjord

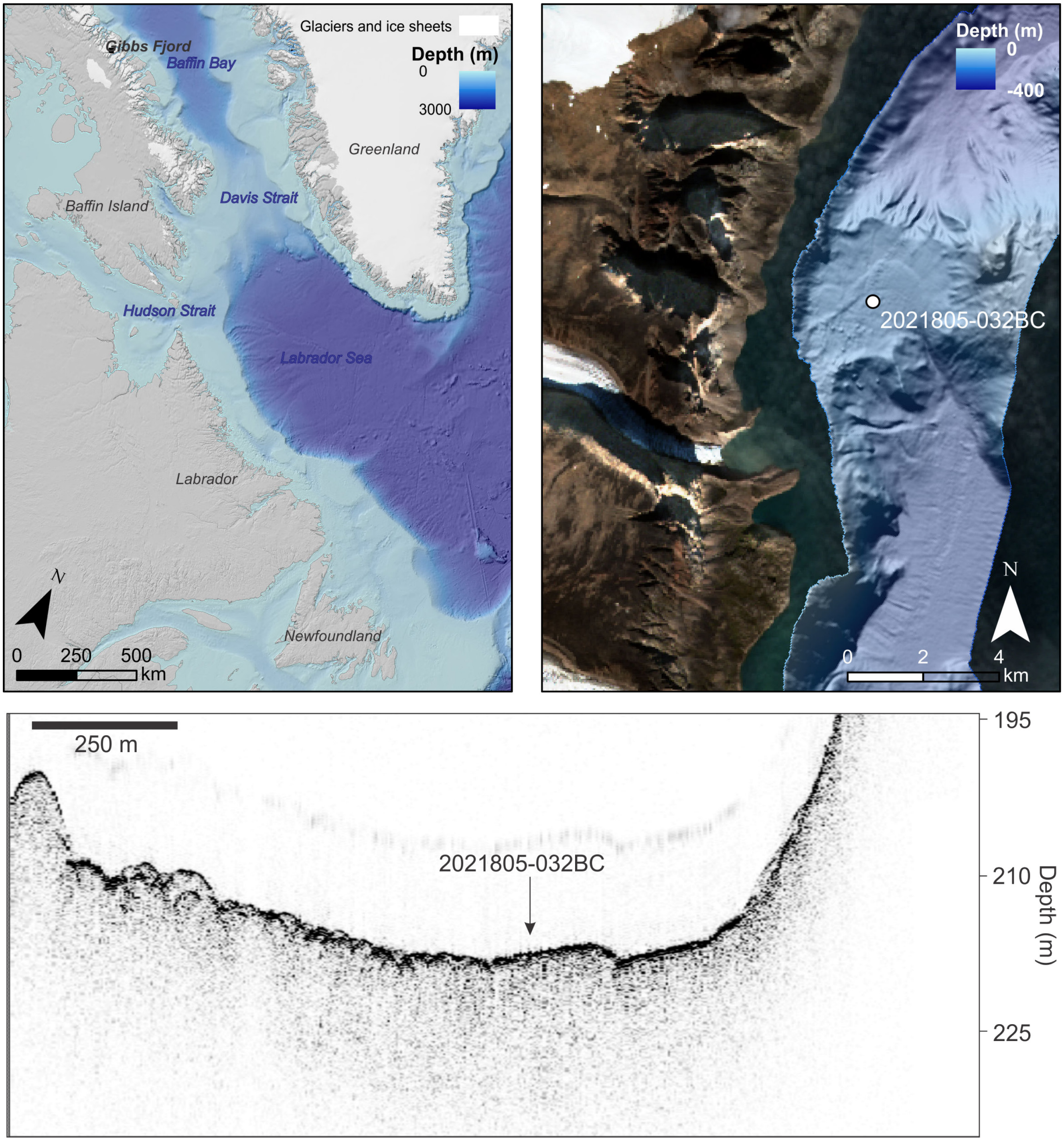

Figure B28: Location of core 2021805-032BC in Clark Fjord

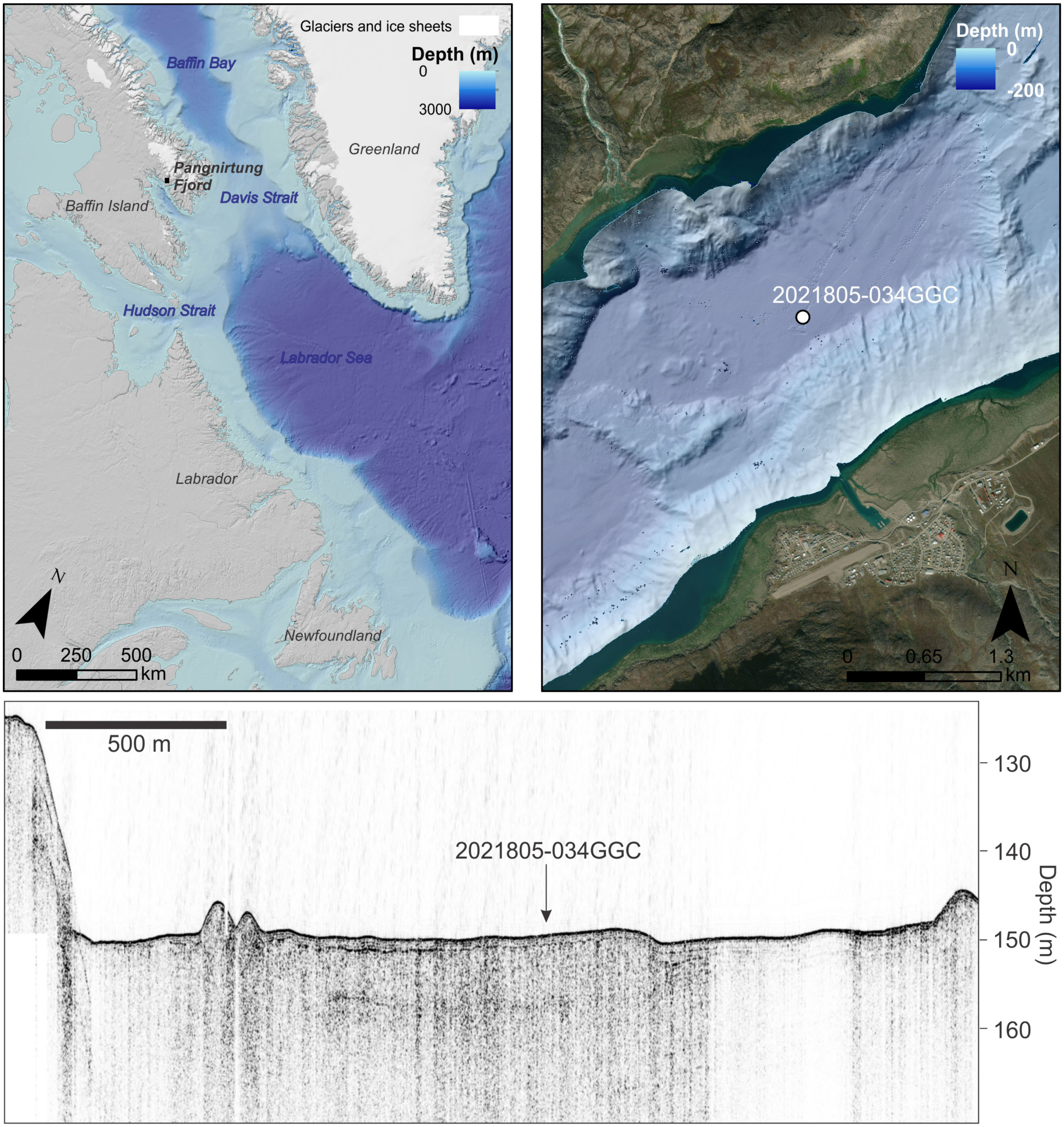

Figure B29: Location of core 2021805-034GGC in Pangnirtung Fjord

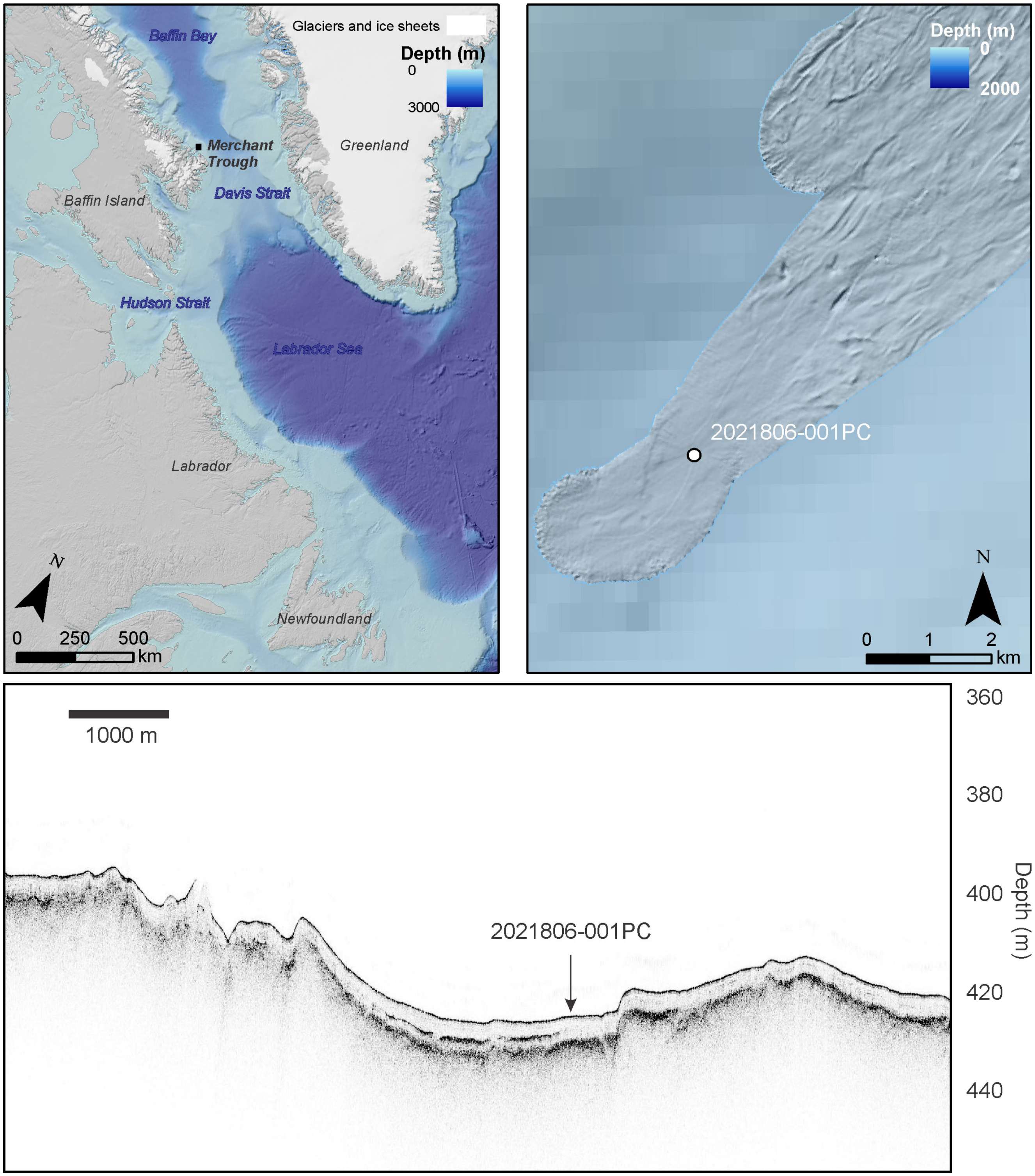

Figure B30: Location of core 2021806-001PC in Merchant Trough

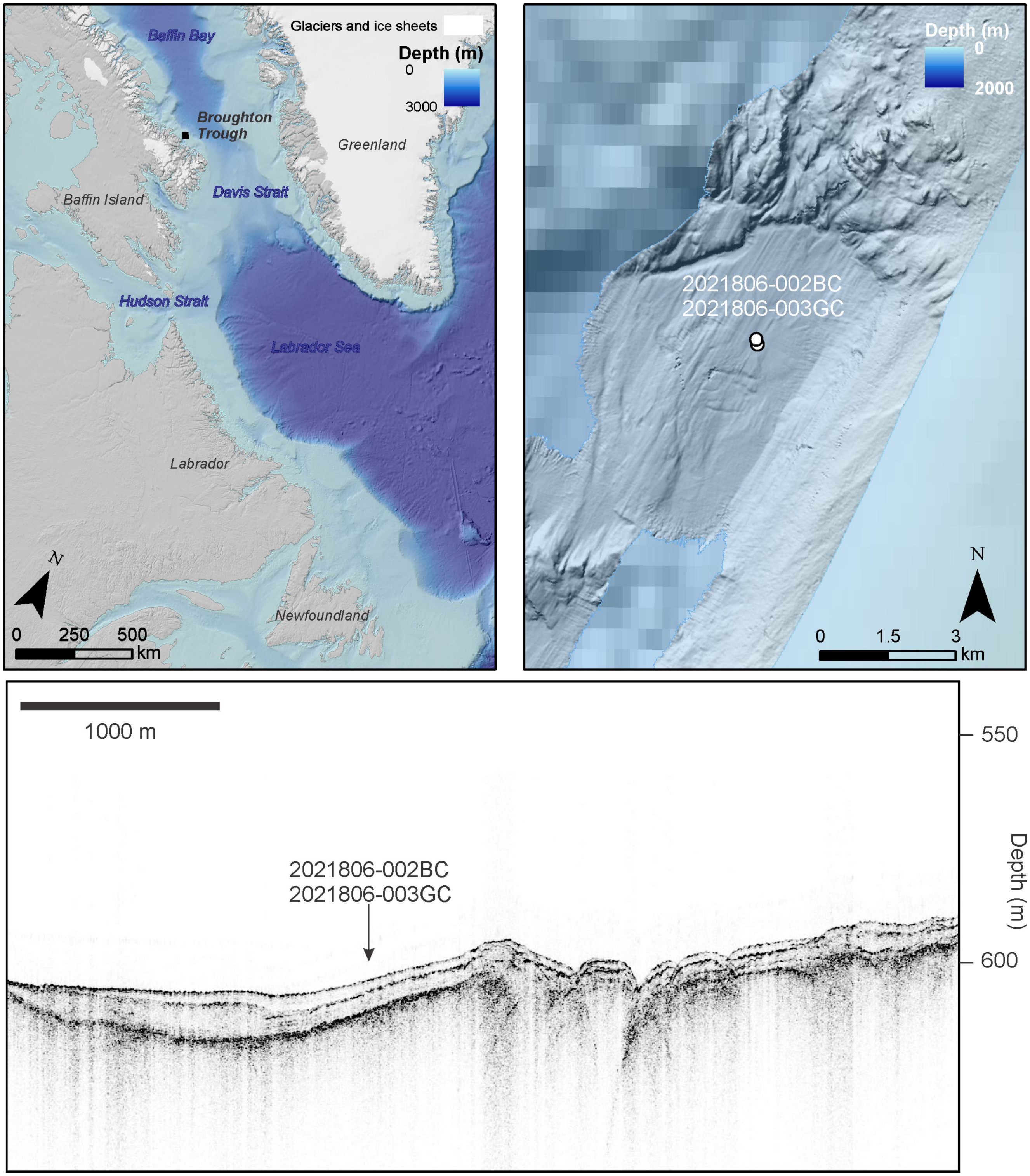

Figure B31: Location of cores 2021806-002BC-003GGC in Broughton Trough

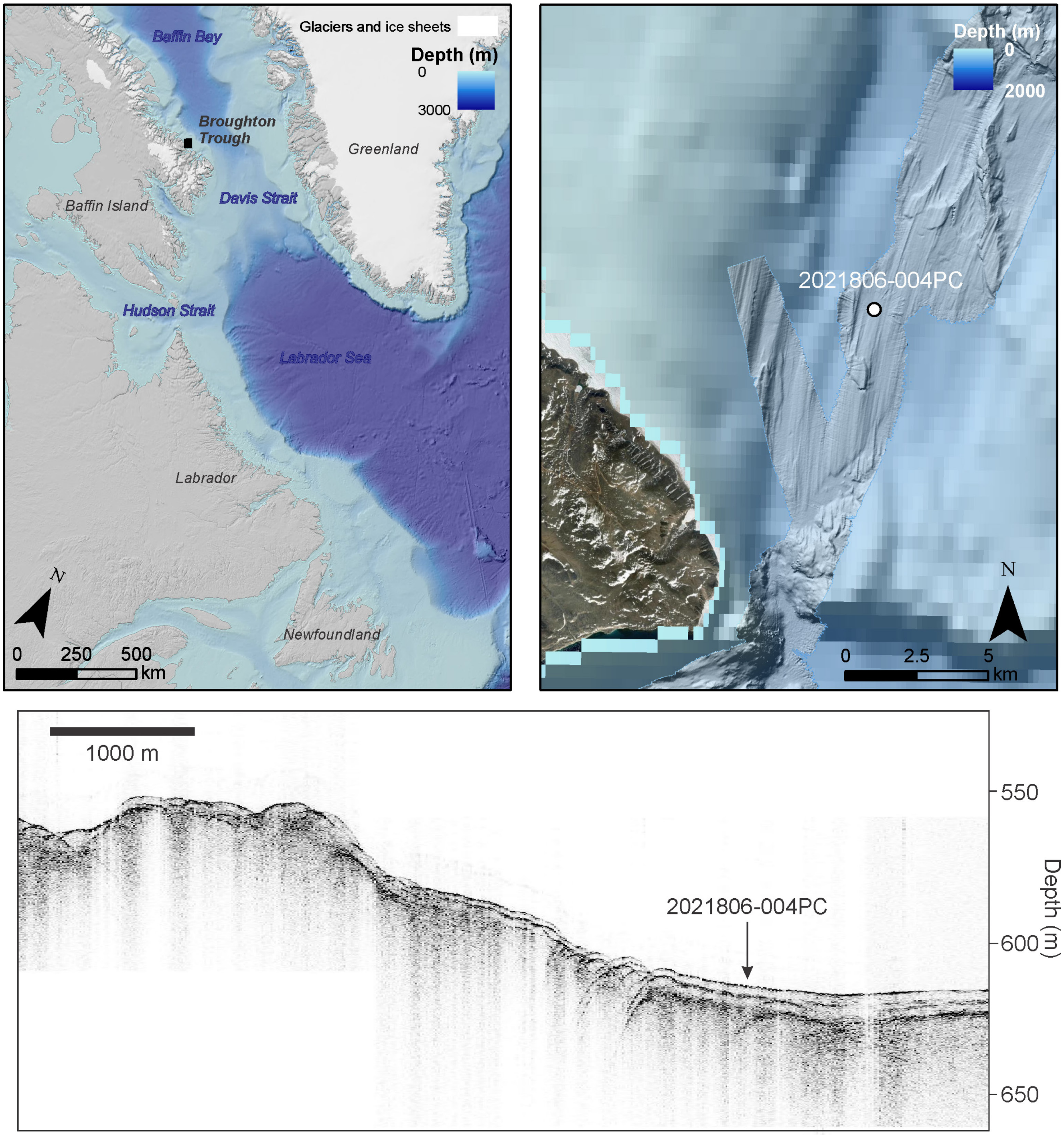

Figure B32: Location of cores 2021806-004PC in Broughton Trough